Contract No:

This document was prepared in conjunction with work accomplished under Contract No. 89303321CEM000080 with the U.S. Department of Energy (DOE) Office of Environmental Management (EM).

Disclaimer:

We put science to work.™

Savannah River National Laboratory®

OPERATED BY SAVANNAH RIVER NUCLEAR SOLUTIONS

A U.S. DEPARTMENT OF ENERGY NATIONAL LABORATORY • SAVANNAH RIVER SITE • AIKEN, SC

Hanford Double Shell Waste Tank Corrosion Studies- Final Report FY2021

P. K. Shukla

R. E. Fuentes

B. J. Wiersma

August 2022

SRNL-STI-2022-00195, Revision 0

SRNL.DOE.GOV

DISCLAIMER

Printed in the United States of America

Prepared for
U.S. Department of Energy

SRNL-STI-2022-00195
Revision 0

Keywords: *Example keywords*

Retention: *Varies*

Hanford Double Shell Waste Tank Corrosion Studies- Final Report FY2021

P. K. Shukla
R. E. Fuentes
B. J. Wiersma

August 2022

Savannah River National Laboratory is operated by Battelle Savannah River Alliance for the U.S. Department of Energy under Contract No. 89303321CEM000080.

REVIEWS AND APPROVALS

AUTHORS:

P. K. Shukla, Applied Materials Research, SRNL Date

R. E. Fuentes, Separation and Sciences Engineering, SRNL Date

B. J. Wiersma, Applied Materials Research. SRNL Date

TECHNICAL REVIEW:

J. T. Boerstler, Applied Materials Research, SRNL Date

APPROVAL:

J. Manna, Director, Materials Technology and Energy Sciences Division, SRNL Date

J. S. Page, WRPS Tank and Pipeline Integrity Date

R. J. Nelson, WRPS Program Manager Date

ACKNOWLEDGEMENTS

The authors want to acknowledge the technical support of T. Murphy and B. Hill in helping perform experiments and characterizations. Preparation of the AZ-101 sludge simulant for the underdeposit corrosion testing was performed by M. Siegfried and D. Jones. Guidance from the WRPS Double Shell Tank Integrity Expert Panel Corrosion Sub-group was appreciated to help achieve completion of tasks.

EXECUTIVE SUMMARY

For fiscal year (FY) 2021, the Savannah River National Laboratory (SRNL) focused on two experimental tasks related to Hanford Double Shell Tank (DST) chemistry and integrity. The first task focused on understanding risk of corrosion due to formation of either continuous layers or discrete patches of deposits on the tanks' inner sidewalls and bottoms. The second task studied vapor space corrosion (VSC) inhibition of the secondary liner using vapor corrosion inhibitors (VCIs) at dosages less than the manufacturer recommended and a control test in which no VCIs were added. Conclusions for activities and experimental tasks that were performed for FY21 supporting Hanford DSTs are presented below in subsections.

1.1 Underdeposit Corrosion Testing

Simulated AZ-101 sludge was prepared, and a method was developed to deposit a dry, adherent sludge layer on the metal coupon surfaces. Electrochemical monitoring utilizing open circuit potential (OCP) and electrochemical impedance spectroscopy (EIS) measurements indicated that the initial adherent, dry sludge layer is not stable after approximately 1 month. Subsequently, the inhibited liquid, which simulated the presence of free liquid in the tank, has free access to the metal surface and passivates the surface. The initial decrease in the OCP for tests with adherent sludge did correlate with the presence of micropits on the coupon surface. However, after approximately 1 month the OCP began to increase and assumed a steady more anodic value. It is hypothesized that after the breakdown of the sludge layer, that the micropits were passivated. Tests that were performed with loose sludge showed no evidence of micropits and OCP measurements indicated that the potential increases in the anodic direction from its initial value.

1.2 Secondary Liner Corrosion

Vapor corrosion inhibitors (VCI) have been investigated as a potential means for inhibition of corrosion of the exterior of the secondary liner. VCI-B has previously been shown to effectively mitigate vapor space corrosion at concentrations that are at 50% of the recommended dosage. In FY21, testing with 25% of the recommended VCI-B dosage showed that the inhibitor ceases to be in effective at the 25% level. Based on previous results from testing in FY19 and FY20, the threshold minimum dosage for VCI-B is between 25 and 50% of the recommended dosage. In practice, if the concentration of VCI-B decreased below 50%, it is likely that replenishment of the VCI would be necessary.

Determining migration rates of the VCIs is critical to field implementation of the VCI technology. It was hypothesized that corrosion potential data can be used to study and determine migration of VCIs. A Pt-wire embedded in each coupon assembly was used as reference for the vapor space and immersed phase coupons in GW + VCI-B and GW only electrolytes. A saturated calomel electrode was also used as the reference for the immersed coupons. The immersed coupons' corrosion potentials in GW + VCI electrolyte were distinctly different compared to GW only electrolyte, when measured with respect to the saturated calomel electrode. However, the corrosion potentials of the immersed Pt wires in the two electrolytes overlapped, indicating that Pt wires' potentials were not steady, and Pt wires could not be used as references to measure corrosion potentials of the coupons. Although accurate potential data were not gathered from this test, corrosion rates from 6-month tests with carbon steel exposed to GW+VCI-B and GW only simulants were able to be compared. The results indicated that there is nearly a 10- to 20- fold decrease in the surface average corrosion rate and a 5- to 10- fold decrease in the pitting rate. This result again emphasizes the effectiveness of the VCIs in mitigating corrosion.

The coupling current tests showed that a distributed concentration of the VCIs under the tank bottom is not likely to result in enhanced corrosion. The corrosion rate of carbon steel in the GW simulants has been observed to be in the range of 3-5 mpy. The coupling current data in general show that the rates are much

less than in the presence of no VCI. Thus, a distributed concentration of the VCIs under the tank bottom is not likely to result in enhanced corrosion.

1.3 Recommendations for FY22 Testing

Recommendations for follow-on work are summarized below. These recommendations were incorporated into a proposal for FY22 activities.

Underdeposit Corrosion

- Investigate underdeposit corrosion under the non-porous adherent deposits considering the effect of water content.

Secondary Liner

- Explore alternative corrosion mitigation methods such as nitrogen blanketing that will effectively de-aerate the system.

TABLE OF CONTENTS

LIST OF TABLES

LIST OF FIGURES

LIST OF ABBREVIATIONS

ASTM	American Society for Testing and Materials
CPP	Cyclic Potentiodynamic Polarization
DNV	Det Norske Veritas
DST	Double-Shell tank
EDM	Electrical Discharge Machine
ER	Electrical Resistance
FY	Fiscal Year
GW	Ground Water
LCM	Laser Confocal Microscope
LDP	Leak Detection Pit
MIC	Microbiologically Influenced Corrosion
mpy	mils per year
NDE	Non-Destructive Examination
NPH	Normal Paraffin Hydrocarbon
OCP	Open Circuit Potential
PF	Pitting Factor
PTFE	Polytetrafluoroethylene
SCC	Stress Corrosion Cracking
SCE	Saturated Calomel Electrode
SRNL	Savannah River National Laboratory
SST	Single-Shell Tank
TAPI	Tank and Pipeline Integrity
TBP	Tributyl Phosphate
TIEP-CSG	Tank Integrity Expert Panel-Corrosion Sub-Group
TOC	Total Organic Carbon
VCI	Vapor Corrosion Inhibitor
VSC	Vapor Space Corrosion
WRPS	Washington River Protection Solutions
WTP	Waste Treatment and Immobilization Plant

2.0 Introduction

The Hanford Site in Washington State has millions of gallons of legacy radioactive waste that is being retrieved from single-shell tanks (SSTs) and transferred to newer, double-shell tanks (DSTs) for eventual closure of SSTs. The waste will be maintained in DSTs until eventual immobilization can be performed at the Waste Treatment and Immobilization Plant (WTP), currently under construction. A detailed integrity program plan, implemented by Washington River Protection Solutions (WRPS) Tank and Pipeline Integrity (TAPI) organization, has been developed for the DSTs, which has many elements including waste chemistry control for corrosion mitigation, visual inspections and non-destructive examination (NDE) of tank walls.

Corrosion testing for DSTs has been guided by the Tank Integrity Expert Panel-Corrosion Sub-Group (TIEP-CSG) to provide the technical guidelines for the corrosion control program. Corrosion testing has been performed at three independent laboratories: Det Norske Veritas (DNV), Savannah River National Laboratory (SRNL), and the 222-S facility at Hanford operated by WRPS. SRNL has focused its corrosion studies on vapor space corrosion (VSC), development of corrosion chemistry limits to mitigate pitting corrosion, and corrosion protection for the DST secondary liner.

For fiscal year (FY) 2021, SRNL focused on two experimental tasks. The first task focused on understanding risk of corrosion due to formation of either continuous layers or discrete patches of solids on the tanks' inner sidewalls and bottoms. The second task studied VSC of the secondary liner using vapor corrosion inhibitors (VCIs) at dosages less that the manufacturer recommended dosages and a control test in which no VCIs were added. The VCI formulation was applied at the mid-point of the experiment to determine its performance on weathered coupons.

3.0 Background

The Task Technical and Quality Assurance Plan (TTQAP) for DST corrosion testing in FY21 included 4 activities [1]. Of the 4 activities, two were experimental studies performed at SRNL. A background is provided below for these two tasks.

3.1 Underdeposit/Crevice Corrosion Studies

Formation of saltcake and scale-like deposits on the wall and the bottom of several Hanford DSTs have been observed; this is based on the loose, small particulate solids in core samples taken from the tanks and post retrieval inspection of the inner surface of the primary tank of AY-102. These solids may promote underdeposit corrosion, which occurs when the liquid above the solids layer seeps in between the solids and the metal surface and creates an aggressive local environment. The objective of this task was to determine the effect of solid deposits on the corrosion risk to the tank bottom, and whether a combination of scale, saltcake and loose solids lead to underdeposit corrosion. In particular, a case where historically high waste temperatures were observed was investigated. The potential for deposition of an adherent solids layer in this environment, and the risk of corrosion beneath the layer, was tested. Double-shell tank AZ-101 was selected as a representative tank for this activity.

AZ-101 was constructed between 1970-74 and was placed into service in 1976 [2]. The tank level history is depicted in Figure 3-1. The service history for the tank may be divided into three historical intervals [2]. Between 1976-1983, the tank received waste from four sources: Evaporator Feed, Double Shell Slurry Feed, Complexed Waste and Non-Complexed Waste. A small amount of solids precipitated on the tank bottom

during this period. After the waste was decanted to DST AW-102, between 1983-1989, the tank received Neutralized Current Acid Waste (Purex) from DST AY-102 and AW-101. Figure 3-2 shows that the waste temperatures approached the boiling point (~215 °F). The air circulators were used to suspend the solids, however, there was solids build-up due to settling of aluminum phases. Since that time there has been only one transfer into or out of the tank (i.e., Tank AN-106 sent a waste transfer in 2009). The temperature has been steady at approximately 145 °F. The air circulators have not been operated during this time so that the solids layer, which is 1-2 feet deep, has been undisturbed.

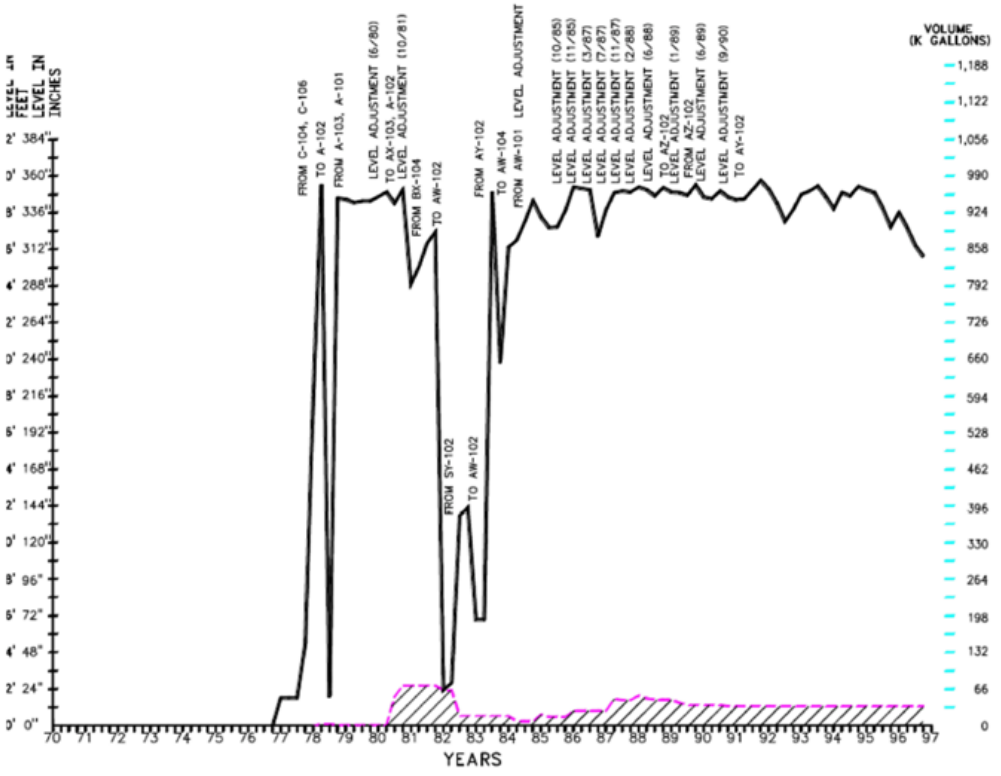

Figure 3-1 Tank AZ-101 Waste Level History from 1976 to 1998.

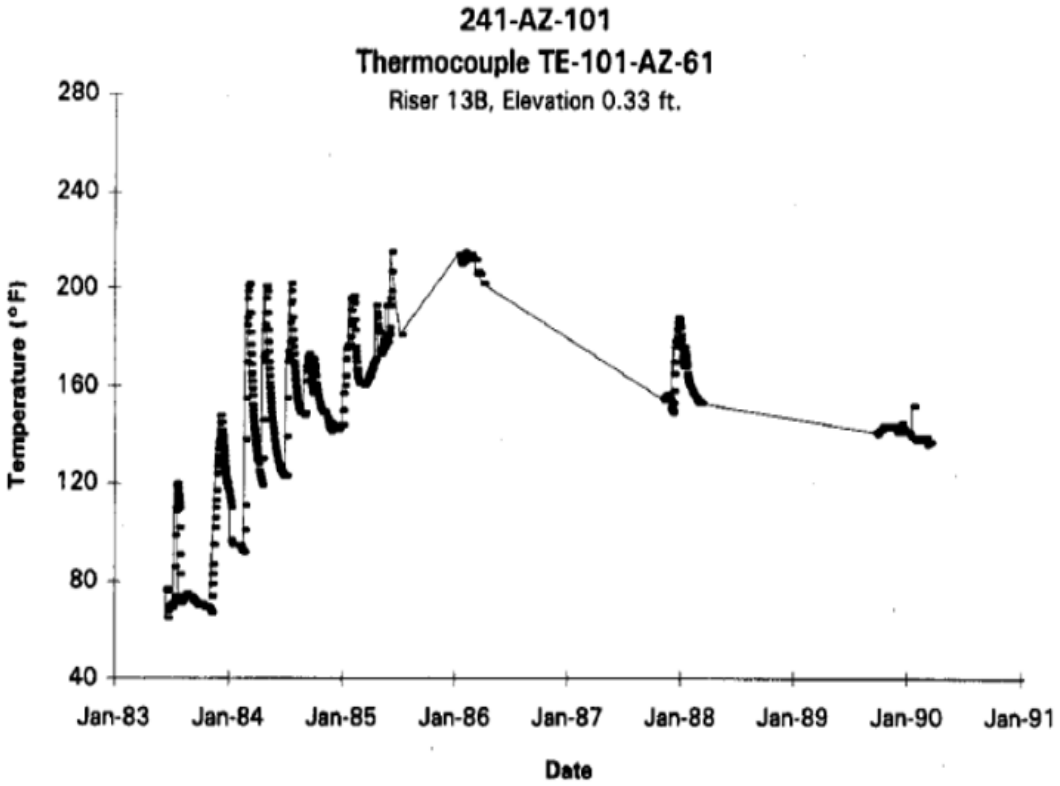

Figure 3-2 Tank AZ-101 Temperature History from 1983 to 1990.

3.2 Secondary Liner Corrosion

Each DST consists of a primary liner (inner) surrounded by a secondary (outer) liner. The secondary liner rests on a concrete foundation that contains slots to direct any leakage to drain slots, which empty to a leak detection pit (LDP) [2], as shown in the schematic in Figure 3-3. Figure 3-4 shows the drain slots that were cast into the foundation of Tanks AZ-101 and AZ-102.

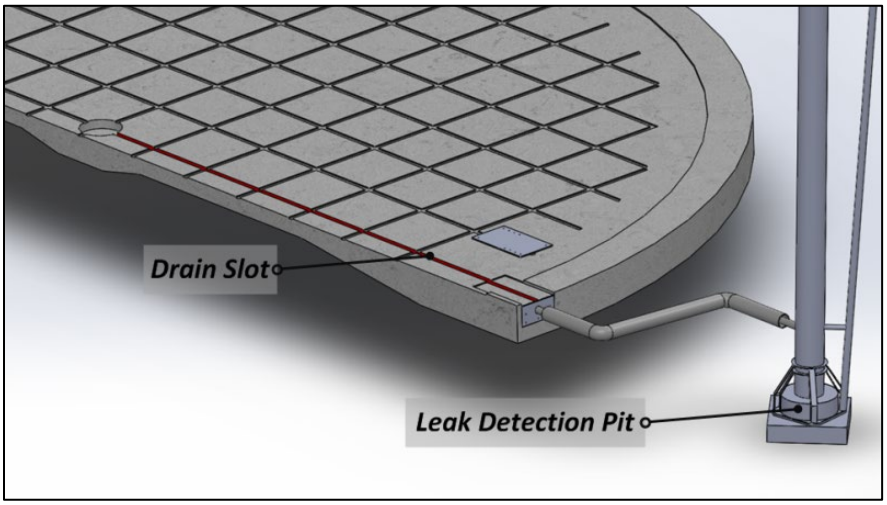

Figure 3-3 Schematic of drain slots connected to the leak detection pit

Figure 3-4 Concrete foundation for tanks AZ-101 (foreground) and AZ-102 (background) showing the cast drain slots.

In 2014 during ultrasonic (UT) inspection of the annulus floor in AP-102, significant material loss was observed [3]. The attack was determined to be on the exterior of the secondary liner in the gap between the liner and the concrete foundation. Since then, similar wall loss, although not as significant, has been observed in other DSTs [3]. Ultrasonic inspection is confined to the annular space between the primary and secondary tanks due to access limitations, leaving a concern that corrosion is widespread on the underside of the secondary liner bottom plate.

Water is known to accumulate in the LDP, and by association presumably in the drain slots, and may induce corrosion on the exterior of the secondary liner. Since the water level can vary in the drain slots, corrosion could be caused by direct contact with the accumulated water, or when the water level is below the underside of the tank bottom, vapor space corrosion (VSC) could also occur. Accumulated water is drained through the slots into LDPs. The drained water was analyzed for its constituents, and two simulants were developed considering the chemical composition range of the accumulated water. The simulants were identified as LDP water and ground water (GW).

Testing with LDP and GW simulants for legacy carbon steel corrosion was started in FY14 with a long-term immersion experiment in which the deleterious effects of these chemistries were observed, with mass loss corrosion rates obtained of approximately 10 mils per year (mpy) [4, 5]. During FY16 testing was focused on the inhibition strategies using commercial vapor corrosion inhibitors (VCI) from Cortec Corporation to coat the samples and minimize VSC and other types of corrosion [6]. Testing continued during FY17, and it was observed that by coating the samples with VCI, the corrosion inhibition was short-lived and did not significantly reduce carbon steel corrosion [7].

In FY18, the VCI recommended dosages investigated were [8]:

- VpCI-645 + VpCI-609 solution with 10% VpCI-609 by weight of solution (100 g VpCI-609 in 1 liter) and 0.75% VpCI-645 by volume (7.5 mL/L), and
- VpCI-337 – 10% solution, i.e., 100 mL in VpCI-337 plus 900 mL of water for 1 L of the VCI solution

The VCIs were directly added to the groundwater solution at the start of the tests. The carbon steel coupons were immersed in the solution and, also, suspended in the vapor space of the corrosion cells. The study results indicated that both VCIs, i.e., VpCI-645 + VpCI-609, and VpCI-337, are effective in mitigating corrosion. However, one vapor space coupon in VpCI-337 environment exhibited pitting corrosion, but none in VpCI-645 + VpCI-609. This suggests that the VpCI-645 + VpCI-609 combination is slightly more effective than VpCI-337 alone in mitigating corrosion, although more tests are needed to confirm [8].

In FY19, the VCI recommended dosages investigated were [9]:

- VCI-A: VpCI-337 – 10% v/v solution in GW simulant, i.e., 100 mL in VpCI-337 plus 900 mL of GW for 1 L VCI formulation.
- VCI-B: 10% wt. VpCI-609 in GW simulant (100 g VpCI-609 in 1 liter) and 0.75% v/v VpCI-649MF (7.5 mL/L)

VCIs formulations were added after two months of exposure to the GW simulant. Three tests were conducted using VCI-A and VCI-B. It should be noted that VCI-B is a new formulation. This formulation eliminated ferric hydroxide precipitates that were observed during the FY18 tests. The first two tests were conducted using 100% recommended dosages of VCI-A and VCI-B. The third test was conducted at 10% of the recommended dosage of VCI-B. The following conclusions are made from the experimental data and results:

- The corrosion rate data indicated that 10% of the recommended dosage of VCI-B is insufficient in mitigating corrosion. This observation is consistent with a prior study which also concluded that VCIs' effectiveness vanishes at 10% of the recommended dosages for the aboveground tank bottom underside application [10].

- The data also showed that 100% recommended dosages of VCI-A and VCI-B mitigated pitting corrosion of weathered coupons. Specifically, VCI-A mitigated pitting corrosion in immersed, Level 2, and Level 3 coupons, whereas VCI-B mitigated pitting corrosion in immersed, Level 1, and Level 3 coupons (See Section 5.3.3 for discussion of Levels in the Vessel). Statistical significance of corrosion rate decrease in Level 1 coupons for 100% recommended dosage of VCI-A and Level 2 coupons for 100% recommended dosage of VCI-B could not be established; this may be due to coupons' surface orientation being vertical during the tests, leading to limited and uneven weathering during GW simulant only and GW simulant plus VCI exposures [9].

- After 2 months of exposure to the vapor space above the GW simulant (i.e., no VCI), the surface average corrosion rates were approximately 6.8 mpy and 2.5 mpy for the immersed and vapor space coupon, respectively. Significant pitting corrosion was also observed.

In FY20, the VCI recommended dosages investigated were [11]:

- VCI-A: VpCI-337 – 10% v/v solution in GW simulant, i.e., 100 mL in VpCI-337 plus 900 mL of GW for 1 L VCI formulation.
- VCI-B: 10% wt. VpCI-609 in GW simulant (100 g VpCI-609 in 1 L) and 0.75% v/v VpCI-649MF (7.5 mL/L)

The VCIs formulations were added after 2 months of exposure to the vapor space above the GW simulant. The tests on the corroded coupons were continued for an additional 4 months. Three tests were conducted using VCI-A and VCI-B. The first two tests were conducted using 100% recommended dosages of VCI-

A and VCI-B. The third test was conducted at 50% of the recommended dosage of VCI-B. The following conclusions are made from the experimental data and results:

- Both VCIs were effective in mitigating the pitting corrosion rate for carbon steel coupons immersed in GW simulant and at the Level 2 conditions for the 100% recommended dosages. VCI-B was more effective than VCI-A in mitigating the pitting corrosion rate at Level 3 conditions.
- 50% VCI-B was also effective in mitigating the pitting corrosion rate for coupons that were immersed and at Level 1 conditions. However, a statistical analysis of the pitting corrosion rate data indicated that it was not as effective in mitigating corrosion of the coupons that were above Level 2 conditions.
- After 2 months of exposure to the vapor space above the GW simulant (i.e., no VCI), the surface average corrosion rates were approximately 5.2 mpy and 2.7 mpy for the immersed and vapor space coupon, respectively. Significant pitting corrosion was also observed.

4.0 Task Description and Activities

The tasks and activities that were performed during FY21 are listed and described in the sections below.

4.1 Task 1: Completion of FY20 report

Task 1 was the completion of the FY20 report for worked performed during that FY. The report was completed and issued in July 2021[11]. It included work on New Limits, Underdeposit/Crevice Corrosion Studies, Secondary Liner corrosion testing using VCI formulations and Long-term OCP drift studies of simulants of AY-101, SY-101 and AW-105 waste at three different conditions: Base, Representative and Elevated Total Organic Carbon (TOC) with small-chain organic acid.

4.2 Task 2: New Chemistry Control Limits Implementation and Technical Support

SRNL provided technical advisory services in this support activity. SRNL participated in bi-weekly telecons, which involved preparing updated reports and making oral presentations to the TIEP-CSG. Additionally, SRNL participated in three special sub-group meetings which covered results of G-192 corrosion tests, in-tank potential measurements, and an evaluation of the pitting factor effectiveness. Reports or notes on these meetings are kept by the Chairman of the Tank Integrity Expert Panel. All meetings were virtual. No further description of these events will be presented in this report.

4.3 Task 3: Crevice/Underdeposit Corrosion Beneath Tank Bottom Solids

The results from FY20 study indicated that loose deposits will not promote underdeposit corrosion [11]. For this task then, the focus was put into the formation of adherent, low porosity deposits from AZ-101 including a supernate simulant and an insoluble solid component. The tests were conducted at 75ºC with the following exposure conditions: (i) tank steel without deposits, (ii) tank steel with saltcake as solid deposits spread throughout the coupon surface, (iii) saltcake deposits localized to a small area of a coupon surface, and (iv) tank steel with saltcake and solids that mimic the core sample and localized to a small area on coupon surface.

4.4 Task 4: Secondary Liner Corrosion Testing

Secondary liner corrosion experiments focused on the effectiveness of VCIs to mitigate corrosion of carbon steel immersed in a corrosive solution and in the vapor phase above the solution. Five tests were conducted using legacy carbon steel coupons immersed in a GW simulant and exposed to the vapor phase above the simulant. The first test was started by just using the GW simulant as a control test. For two of other tests, the VCI was added to the GW simulant at 25% and 100% of the recommended dosage. The experiment with 100% of the recommended dosage was also conducted to measure potentials of the coupons so that migration of the VCI through the column could be assessed. The mounted coupon was modified by attaching a wire with silver epoxy for electrical connection and mounted close to a platinum wire to be used as a pseudo reference electrode. These coupons were immersed in solution in the GW simulant and 100% recommended dosage VCI in GW.

5.0 Experimental Procedure

5.1 Materials for Testing

The material used for all corrosion testing was carbon steel selected from AAR TC-128 Rail Car Steel. This steel was selected for testing since it approximates the chemistry and microstructure of American Society for Testing and Materials (ASTM) A515, Grade 60 carbon steel, the steel from which the DSTs in AY-Farm and AZ-Farm were fabricated [12]. The chemical composition of the steel is shown in Table 5-1.

Table 5-1 Chemical Composition of AAR TC-128 Rail Car Steel

	C	Mn	P	S	Si	Fe
Specification (wt.%)	0.24 (max.)	0.9 (max.)	0.035 (max.)	0.04 (max.)	0.13 to 0.33	Balance
Measured (wt.%)	0.212	1.029	0.012	0.013	0.061	Balance

5.2 Underdeposit Corrosion Testing

5.2.1 Preparation of AZ-101 Interstitial Liquid Simulant

The most recent sample of the interstitial liquid was obtained in 1999 as shown in Table 5-2 [13]. The pitting factor for this composition is on the order of 4.6. Best Basis Inventory compositions are calculated by WRPS to project the anticipated chemistry of the waste over time. The projected chemistry of the interstitial liquid in 2018 is also shown in Table 4-2. The pitting factor had decreased to a value slightly below 2. The modified AZ-101 simulant composition utilized the original sample results as well as the concept that the solution chemistry may become more aggressive (i.e., pitting factor on the order of 2). The sample chemistry was modified by adjusting the hydroxide ion concentration such that the pitting factor is less than 2 [14]. OLI™ was utilized to adjust values for aluminum, sulfate, carbonate, and fluoride in order to minimize precipitation in the simulant. The modified AZ-101 interstitial liquid, as shown in Table 5-22, was utilized for these tests and is considered to be a conservative estimate of the AZ-101 interstitial liquid composition.

Table 5-2 Chemical Composition of AZ-101 Simulant

Source Chemical	1999 AZ-101 Interstitial Liquid Sample (M)	2018 BBI for AZ-101 Interstitial Liquid Sample (M)	Modified AZ-101 (M)
Sodium hydroxide	0.68	0.42	0.0818
propionic acid	NA	NA	0.00075
Sodium aluminate	0.3	7.07	0.025
Sodium fluoride	0.12	0.32	0.120
Sodium nitrite	1.60	1.04	1.60
Sodium nitrate	0.83	0.58	0.826
Potassium nitrate	0.12	0.07	0.12
Trisodium phosphate, 12-hydrate	0.02	0.08	0.020
Sodium sulfate	0.23	0.38	0.050
Sodium carbonate	0.57	1.1	0.570
Sodium chromate	NM	NM	1.00E-03
Boric acid	NM	NM	1.00E-03
Pitting Factor	4.61	1.95	1.91

NM-Not measured. Component was not measured in sample, but necessary for simulant preparation.

5.2.2 AZ-101 Insoluble Solids (Sludge) Simulant Preparation

The FY22 underdeposit corrosion testing was performed utilizing an AZ-101 sludge simulant. The HLW Precipitated Hydroxide nominal simulant preparation was developed by SRNL in 2003 to reproduce the chemical and physical properties of the AZ-101 sample processed by Battelle in 2000 [15, 16]. The simulant was comprised of four major components (Al, Fe, Si, Zr) as hydroxides or as oxides with known particle properties (density and size). Simulant preparation was based on a process designed to mimic the manner the solids precipitated in the waste tank. The principal steps in the recipe are:

1. Generate hydrated manganese dioxide by reacting permanganate ion and manganese (II) ion. The compounds and amounts on a per liter basis are shown in Table 5-3. Fine black solids will be produced in this step.

Table 5-3 Compounds for preparation of hydrated manganese dioxide solids. These are dissolved in 1 liter of water.

Compound	Formula	Mass (g)
Potassium Permanganate	$KMnO_4$	1.913
Manganese Nitrate Solution, 50 wt.%	$Mn(NO_3)_2$	6.60

2. Add the transition metals, lanthanides and alkaline earth metals as nitrates or chlorides to the hydrated manganese dioxide solids. The compounds and the amounts are shown in Table 5-4. All compounds dissolve in the solution except for the manganese dioxide solids. The pH will be approximately 1.3.

Table 5-4 Compounds for transition metals, lanthanides, alkaline earth metals.

Compound	Formula	Mass (g)
Ferric Nitrate	$Fe(NO_3)_3 \bullet 9H_2O$	453.86
Nickel Nitrate	$Ni(NO_3)_2 \bullet 6H_2O$	15.348
Zirconyl Nitrate	$ZrO(NO_3)_2 \bullet 6H_2O$	75.012
Cerium Nitrate	$Ce(NO_3)_3 \bullet 6H_2O$	5.034
Lanthanum Nitrate	$La(NO_3)_3 \bullet 6H_2O$	5.612
Neodymium Nitrate	$Nd(NO_3)_3 \bullet 6H_2O$	4.042
Barium Nitrate	$Ba(NO_3)_2$	0.891
Calcium Nitrate	$Ca(NO_3)_2 \bullet 4H_2O$	13.708
Cadmium Nitrate	$Cd(NO_3)_2 \bullet 4H_2O$	12.335
Chromium Nitrate	$Cr(NO_3)_3 \bullet 9H_2O$	5.450
Cobalt Nitrate	$Co(NO_3)_2 \bullet 6H_2O$	0.195
Cupric Nitrate	$Cu(NO_3)_2 \bullet 2.5H_2O$	0.662
Magnesium Nitrate	$Mg(NO_3)_2 \bullet 6H_2O$	5.036
Lead Nitrate	$Pb(NO_3)_2$	0.856
Rhodium Nitrate	$Rh(NO_3)_3$, Solution with 4.933 wt.% RH	3.221
Ruthenium Trichloride	$RuCl_3$ 41.74 wt.% Ru	1.188
Strontium Nitrate	$Sr(NO_3)_2$	2.554
Zinc Nitrate	$Zn(NO_3)_2 \bullet 6H_2O$	0.391
Silver Nitrate	$AgNO_3$	0.004

3. While measuring the pH of the solution, add 8 M sodium hydroxide to precipitate the metal hydroxides/oxides. The pH should be greater than 10.
4. Add 0.6 M sodium carbonate (approximately 400 ml) to convert the more soluble hydroxides (e.g., calcium and magnesium) to carbonates. The final pH at this step will be approximately 12. The solids are greenish-black as shown in -Figure 5-1.

Figure 5-1 Precipitate solids after the addition of the sodium carbonate.

5. Allow the solids to settle for approximately 2 weeks. During this process the sludge turns from blackish-green to reddish orange (See Figure 5-2), which indicative of the transition from $Fe(OH)_3$ to Fe_2O_3.

Figure 5-2 Change in precipitate solids during settling.

6. Wash the insoluble solids with inhibited water (0.01 M NaOH and 0.01 M $NaNO_2$) to remove excess soluble sodium, nitrate, and carbonate ions. This process is accomplished by a) decanting the liquid layer above the settled solids, b) adding back inhibited water and mixing for approximately 30 minutes, c) allowing the solids to settle and then d) repeating steps a) through c) until the nitrate concentration is approximately 1000 mg/l. Figure 5-3 shows the pump and mixer set-up for the washing the solids.

Figure 5-3 Set-up for washing with inhibited water.

7. At the completion of washing, the liquid above was decanted until the sludge slurry was approximately 10-11 wt.% solids. At this point there was approximately 16 liters of precipitate slurry.
8. Hydroxide-reactive insoluble species of known particle size were added to the 11 wt.% sludge slurry and mixed thoroughly for 30 minutes. The compounds, amounts, and their particles sizes are shown in Table 5-5.

Table 5-5 Metal oxides/hydroxides used in AZ-101 sludge simulant

Material	Product Name	Mass (g)
Aluminum Oxide, 99.5%	Fine Powder	58.5
Silica, SiO_2	Silicon (IV) Oxide, 99.5%, -400 mesh	8.66
Tin (IV) Oxide	Tin (IV) Oxide, -325 Mesh, 99.9%	1.42
Titanium Dioxide	Titanium (IV) Oxide < 5 µm, 99.9%	0.092

9. The sludge slurry was placed in a heated vessel with a condenser. The slurry was boiled at 102-103 °C for 6 to 7 hours to raise the total insoluble solids concentration to greater than 20%. Figure 5-4 shows the sludge slurry before and after the concentration step. A close-up of the sludge slurry simulant is shown in Figure 5-5. Approximately 8 liters of sludge was prepared for these tests. The process took approximately 45 days.

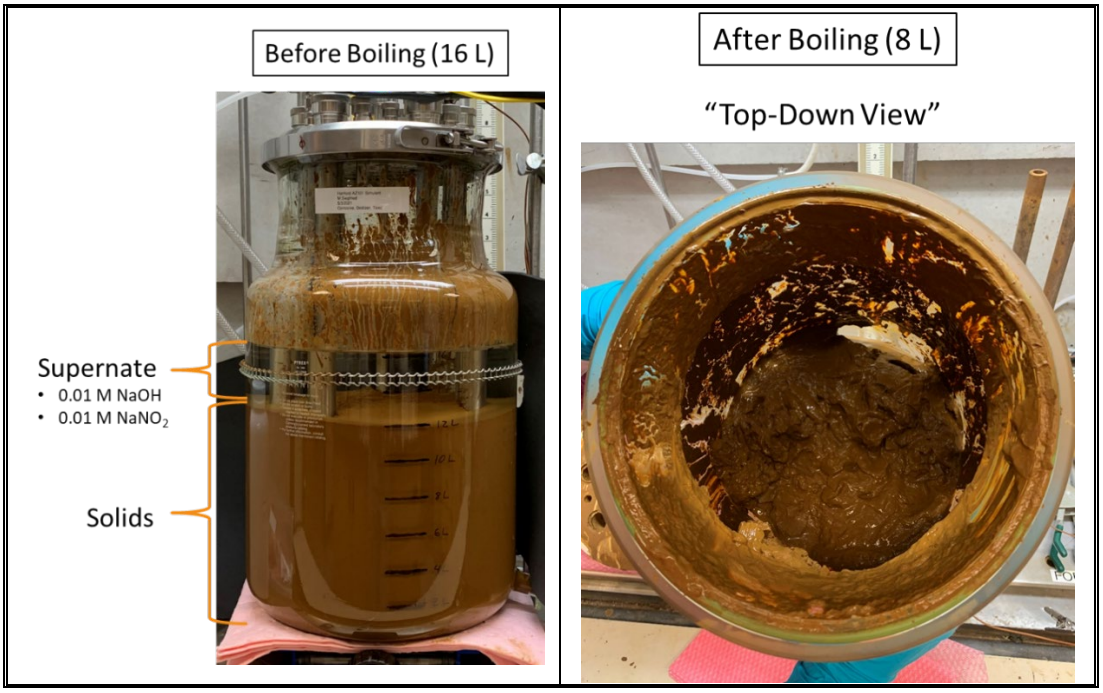

Figure 5-4 Sludge slurry as it is evaporated.

Figure 5-5 Final sludge slurry product.

An SEM micrograph of the undissolved solid particles is shown in Figure 5-6. The final sludge slurry was also characterized for particle size, wt.% solids, and sludge slurry density. These values were compared to the same values that were measured for the 2000 AZ-101 core sample and the 2003 SRNL simulant that was produced. The particle size distribution for each sludge slurry is shown in Figure 5-7. The distributions are presented two ways: a) percentage in a channel (i.e., for a given diameter, the percentage of the total number or volume that are at that diameter.) and b) the cumulative distribution of particle size diameter. The 50th percentile diameter for each was compared and is shown Table 5-6. In addition, the wt.% insoluble solids and the sludge slurry density are also shown in the table. The 50th percentile for the 2021 sludge simulant was approximately 8.3 µm, whereas the 50th percentile for the actual 2000 sludge was approximately 3.3 µm. The distributions indicate that there were several large solids particles (~100 µm) present in the 2021 sludge, whereas there were no particles sizes greater than 30 µm measured for the 2000 sludge. It is possible that some particle agglomeration occurred with the 2021 sludge. Particle agglomeration seems even more likely with the 2003 SRNL simulant. In this case the 50th percentile particles size was nearly 25 µm, and large particles near 250 µm were measured.

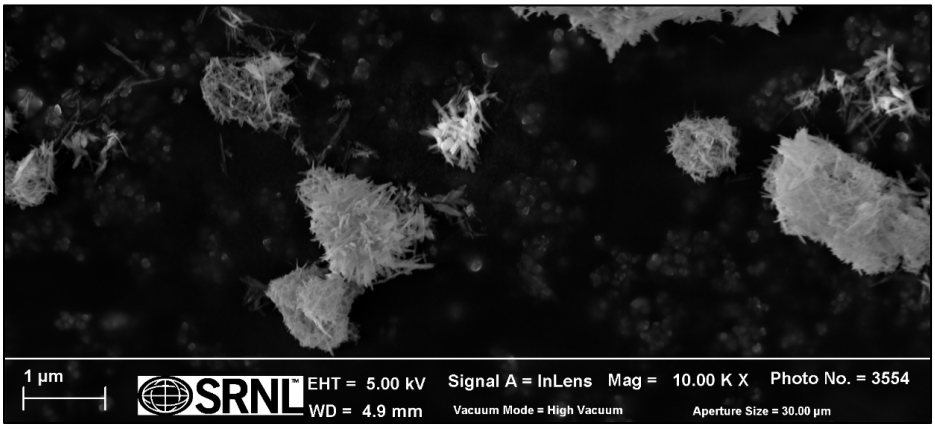

Figure 5-6 SEM micrograph of sludge particles.

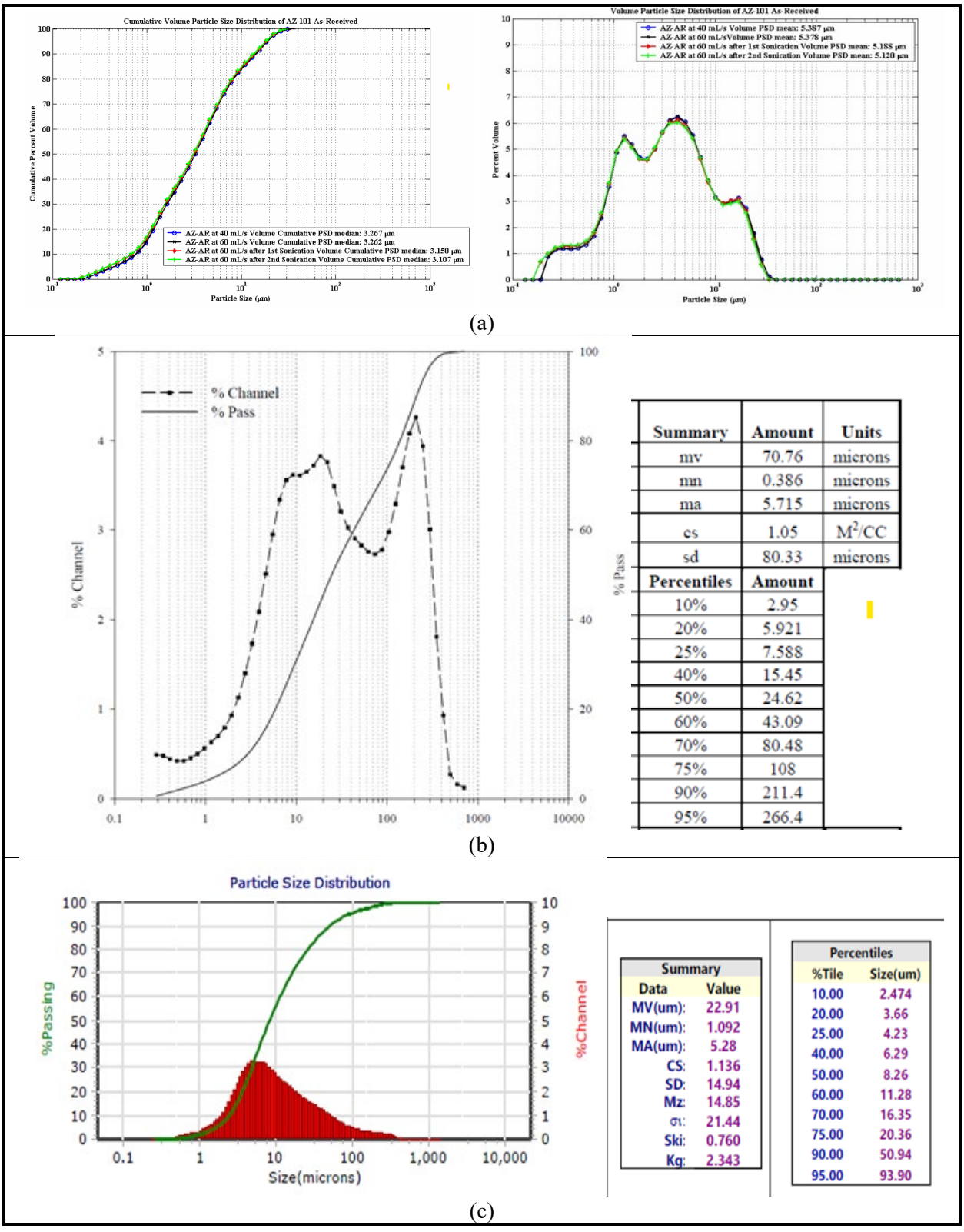

Summary	Amount	Units
mv	70.76	microns
mn	0.386	microns
ma	5.715	microns
cs	1.05	M^2/CC
sd	80.33	microns

Percentiles	Amount
10%	2.95
20%	5.921
25%	7.588
40%	15.45
50%	24.62
60%	43.09
70%	80.48
75%	108
90%	211.4
95%	266.4

Summary	
Data	Value
MV(um):	22.91
MN(um):	1.092
MA(um):	5.28
CS:	1.136
SD:	14.94
Mz:	14.85
σι:	21.44
Ski:	0.760
Kg:	2.343

Percentiles	
%Tile	Size(um)
10.00	2.474
20.00	3.66
25.00	4.23
40.00	6.29
50.00	8.26
60.00	11.28
70.00	16.35
75.00	20.36
90.00	50.94
95.00	93.90

Figure 5-7 Particle size distributions for a) 2000 core sample of AZ-101, b) 2003 AZ-101 sludge simulant, and c) 2021 AZ-101 insoluble solids simulant

The evaporation step concentrated the sludge slurry and was designed to achieve a similar wt.% solids and sludge slurry density that was measured for the 2000 core sample. Table 4-5 shows that these parameters for the sludge simulants compare very well with that of the actual sample.

Table 5-6 Comparison of Sludge Slurry Parameters

Sludge	50% Particle Size (µm)	Sludge Slurry Density (g/ml)	Wt.% Solids
2000 AZ-101 Core Sample	3.3	1.25	25.6
2003 AZ-101 SRNL Sludge Simulant	24.62	1.22	25.8
2021 AZ-101 SRNL Sludge Simulant	8.26	1.23	25.1

5.2.3 AZ-101 Adherent Insoluble Solids (Sludge) Preparation

Corrosion beneath adherent insoluble solids (i.e., sludge) on a carbon steel surface was investigated. Initially, a process for preparing an adherent sludge layer was developed. After consultation with sludge preparation experts at SRNL [17], evaporation of the sludge simulant mixed with excess free supernate was recommended. Additionally, the experts had observed excess aluminum species present in adherent solids that formed on metal surfaces in the laboratory. Thus, excess sodium aluminate was also added to the mixture.

The proportions for the compounds employed for the adherent sludge layer were: 1 mL of AZ-101 supernate simulant; 0.0184 g sodium aluminate; 0.1 g AZ-101 insoluble solids. As a test, these proportions were multiplied by 200 (i.e., 200 ml of AZ-101 simulant; 3.68 g of sodium aluminate; 20 g of AZ-101 sludge solids). The vertical hotwall set-up, shown in Figure 5-8, was utilized for evaporation. A 3” diameter carbon steel coupon was connected to the hotwall apparatus. A 2” diameter PTFE cylinder was mounted vertically above the coupon as shown in the figure. Thus, the solids would primarily adhere to the metal surface and not to the sidewall of the cylinder. The hotwall apparatus was operated at a temperature between 110 – 120 ºC. As observed in Figure 5-9, this formulation successfully created an adherent layer on the metal surface that was approximately 0.25” thick. A layer of soluble salts, likely from the AZ-101 supernate simulant and the sodium aluminate, was also present on top of the sludge. The proportions of simulants used in this development stage were subsequently used to prepare a completely covered 3” diameter coupon and a partially covered coupon (approximately 1” diameter).

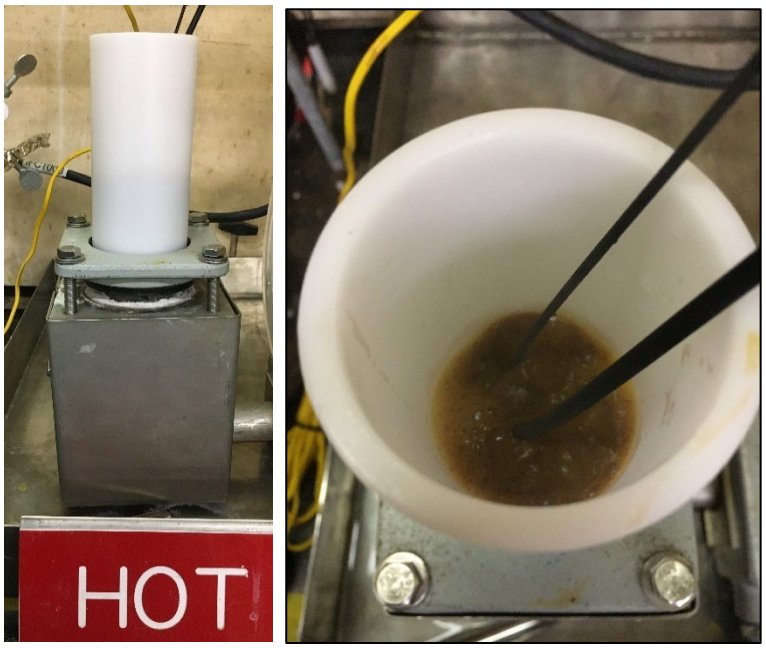

Figure 5-8 Hot wall setup to create adherent insoluble solids layer: (a) show the complete setup and (b) shows inside with the sludge and PTFE coated thermocouples.

Figure 5-9 Adherent insoluble solid baked on a carbon steel coupon

5.2.4 Test Matrix and Set-up

Six vessels were fabricated by the SRNL glass shop for the tests. Figure 5-10 presents front and top view images of one of the vessels. The vessels were approximately 10.5” high and approximately 4” in diameter. Ports were formed on the lid in order to insert electrodes for the electrochemical tests, a thermocouple, a condenser, and finally a port for solution addition, as necessary.

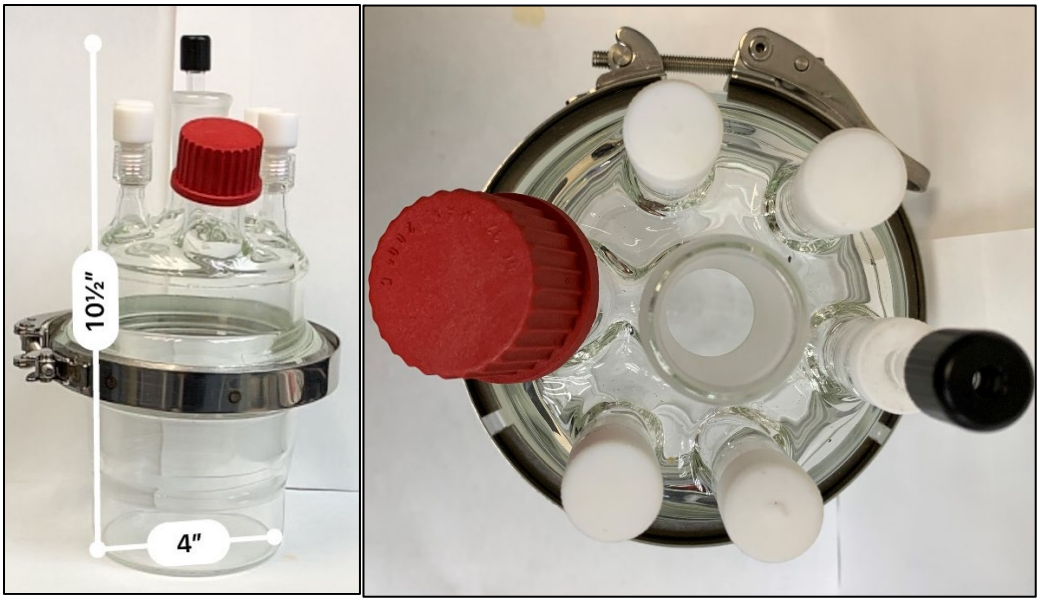

Front view **Top view**

Figure 5-10 Glass vessel used for underdeposit testing: Front view with dimensions at the left; Top view at the right showing the seven different ports on the lid.

The experiments were conducted using a 3" diameter × 0.125-inch thick coupon fabricated from AAR TC 128 steel plate. An insulated wire was attached to the back of the coupon using silver epoxy to provide electrical connection for the electrochemical tests. The coupons were then mounted in a mold prepared with a two-part clear epoxy solution (EpoKwick® from Buehler) so that one face of the coupon was exposed to the test electrolyte. Prior to mounting, each coupon was weighed so that the weight change at the end of the tests could be recorded. A total of six tests were conducted. Details of each test are listed in Table 5-7. All six tests were conducted at 70 °C and atmospheric pressure, with the exposure being for four months. Experiments 1, 2, 5 and 6 used coupons that were polished to a 600-grit finish prior to testing and experiments 3 and 4 used coupons that were pre-corroded by immersing one face of the coupon in GW simulant [18] for approximately two months at room temperature. Figure 5-11 shows coupons 3 and 4 after the immersion, cleaned with de-ionized (DI) water and dried.

To prepare the adherent deposits on the coupons for Experiments 1 to 4, the amount of the sludge-supernate mixture utilized was 300 and 50 times the previously discussed sludge/supernate proportions (see section 5.2.3) for the complete and partial coverage of the coupon, respectively. For example, this meant that for complete coverage of the coupon 300 ml of the sludge-supernate mixture was utilized, while 50 ml was necessary for partial coverage. For the complete coverage coupons (Tests 1 and 3), the mounted coupon was placed inside the vessel and covered with the sludge/supernate mixture and then placed on a hotplate set at 120 ℃. The hotplate was operated for 6 to 8 hours until the layer was dried. For partial coverage of the coupon, the simulant was placed inside a 1" diameter glass ring on top of the mounted coupon. The assembly was then placed in a furnace. After 12-18 hours, the layer was completely dry and was transferred to the vessel with the attached glass ring. Figure 5-12 illustrates the partial and completely covered coupons. Crystal formation was observed on the exterior of the glass ring, which fixed the location of the glass ring during the experiments. For Experiments 5 and 6, the AZ-101 insoluble solids were loosely placed on the surface of the coupon for the complete coverage case and inside the glass ring for the partial coverage coupon. Since the sludge quantities for these two tests are similar to experiments 1-4, these two tests would represent a control experiment.

Table 5-7 Test Matrix for Underdeposit/Crevice Corrosion

Experiment	Deposit Condition	Coupon Condition
1	Adherent AZ-101 insoluble solids deposit completely covering the coupon	600-grit finished coupon
2	Adherent AZ-101 insoluble solids deposit partially covering the coupon	600-grit finished coupon.
3	Adherent AZ-101 insoluble solids deposit completely covering the coupon	Coupon pre-corroded using GW simulant for two months.
4	Adherent AZ-101 insoluble solids deposit partially covering the coupon	Coupon pre-corroded using GW simulant for two months
5	AZ-101 insoluble solids completely covering the coupon (Control)	600-grit finished coupon
6	AZ-101 insoluble solids partially covering the coupon (Control)	600-grit finished coupon.

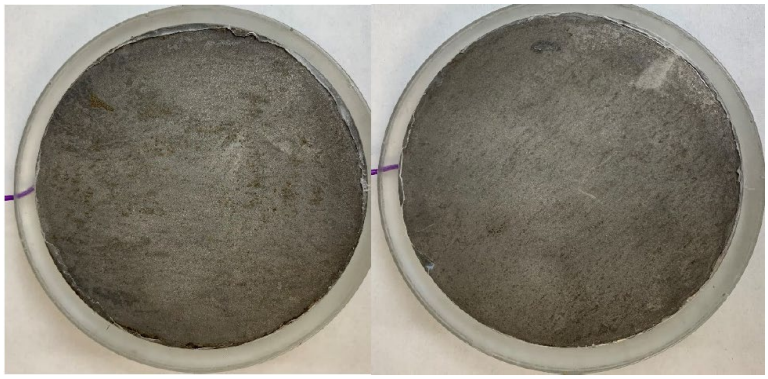

Figure 5-11 Pre-corroded coupons for experiment 3 (left) and experiment 4 (right)

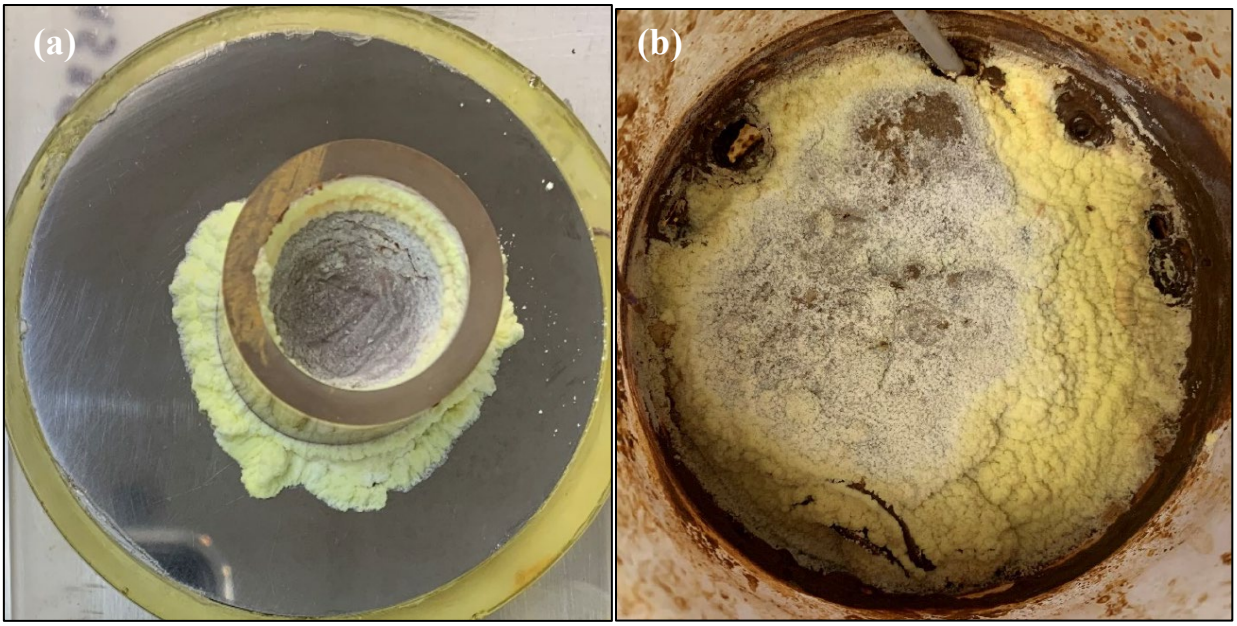

Figure 5-12 Partial covered coupon (Left), completely covered coupon (Right)

For each setup, two vessels on individual hotplates were placed on a secondary container that contains the partial and complete coverage conditions (see Figure 5-13). Approximately 500 ml of the supernate simulant was added to the vessel and the temperature was maintained at 70 ºC. The hotplates were connected to an over temperature controller with an additional thermocouple to ensure the temperature was maintained and stopped if the temperature went outside the maximum limit of 80 ºC. A condenser was placed in the middle port of each container and was connected in series with a chiller that maintained a temperature of 20 ºC to prevent evaporative losses. The tests were conducted for 4 months.

5.2.5 Testing Sequence

The carbon steel coupon was mounted in epoxy and an insulated wire was attached so that it could function as a working electrode. A carbon graphite rod was inserted into the vessel to serve as the counter electrode and a saturated calomel electrode (SCE), which was contained in a salt bridge with a conductive fill solution, was periodically inserted into the liquid so that open circuit potential (OCP) measurements and electrochemical impedance spectroscopy (EIS) tests could be conducted. The OCP was monitored, with a Gamry™ potentiostats, on a frequent basis initially (e.g., daily) to capture the initial transient, but as it became more stable, weekly or bi-weekly measurements were made.

The EIS scans were performed with a BioLogic™ potentiostat. The tests were initiated soon after the coupons were exposed to the liquid and then approximately every two weeks thereafter. The range of frequency was between 10^{-4} to 10^{4} Hz. The focus of the test was to examine the resistance in the higher frequency ranges (i.e., the ohmic resistance).

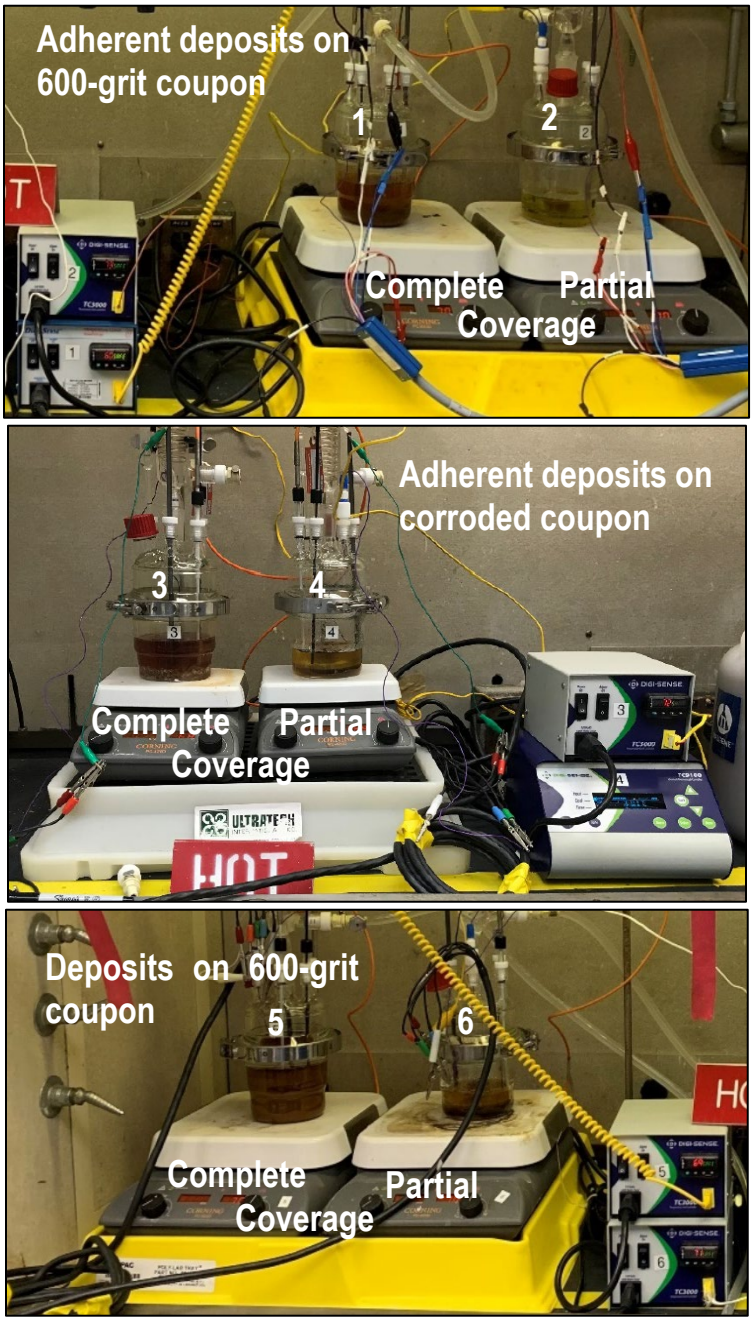

Figure 5-13 Pictures of each test setup illustrating all the conditions tested.

5.3 Secondary Liner Corrosion Testing

5.3.1 Materials

Disk coupons, machined from AAR TC 128 steel plate, were used in the secondary liner experiments. The "base" coupons were 25 mm (1 inch) diameter with a thickness of 3 mm (0.125 inch) and polished to a 600-grit finish. The coupons were mounted in a mold prepared with a two-part clear epoxy solution (EpoKwick® from Buehler) so that one face of the coupon was exposed to the test electrolyte. Prior to mounting, each

coupon was weighed so that the weight change at the end of the tests could be recorded. A crevice former was tightly attached to each coupon surface using tape and wire (see configuration in Figure 5-14). The crevice former partially covered the coupon surface, which created conditions for crevice corrosion. A "modified" version of the coupon included platinum wire that was connected by a wire, as well as a connection of another wire behind the coupon. The modified coupon assembly is presented in Figure 5-15. The wires were electrically connected by applying a layer of silver epoxy to each. The coupons were then mounted in a slightly larger mount than the "base" coupon. This configuration will be known in the text as "modified".

(a) Top view **(b) Side View**

Figure 5-14. (a) Top, and (b) Side views of the partially covered "base" coupon. The coupon's surface is partially covered with a crevice former, which is held in place using purple wire and tape

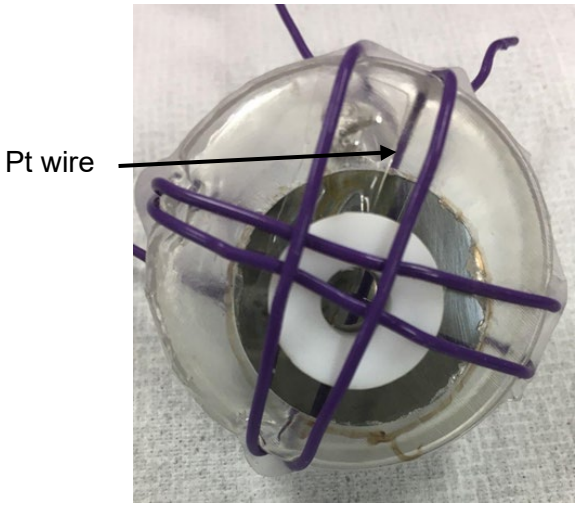

Figure 5-15. Top view of the partially covered coupon in the "modified" mount with platinum wire and Nafion™ film interconnecting the Pt-wire with the metal surface.

5.3.2 Simulants and VCIs

Groundwater (GW) simulant was used for the secondary liner corrosion studies. The composition of the GW simulant is provided in Table 5-8 and is presented in more detail in Appendix A. The pH of the simulant was adjusted using sodium carbonate and acetic acid to a pH of 7.6. A control test was performed with the GW simulant alone. A second test, with the VCI formulation shown in Table 5-9 mixed into the GW simulant, was also performed. A third test with the VCI was performed at 25% of the recommended dosage shown in Table 5-9.

Table 5-8 Composition of GW Simulant

Chemical	Concentration (M)
Sodium bicarbonate	1.750E-03
Calcium hydroxide	1.500E-03
Potassium nitrate	2.400E-04
Strontium Nitrate	2.874E-06
Ferric sulfate	6.250E-04
Sodium Metasilicate, 5-hydrate	6.000E-04
Ferric chloride	7.667E-05
Manganese Chloride	3.100E-04
Acetic Acid	3.000E-04
pH adjusted using sodium carbonate and acetic acid	7.6

Table 5-9 VCI strategy with manufacturer recommended dosage

VCI strategy	VCI product used	Recommended dosage
VCI-B	VpCI-609 and VpCI-649MF	10% wt. VpCI-609 in GW (100 g VpCI-609 in 1 L of GW) and 0.75% v/v VpCI-649MF in GW (7.5 mL in 1 L of GW)

5.3.3 Testing Apparatus

Glass columns that were 3.3 ft tall and 5.5-inch diameter were used for each experiment (see Figure 5-16). Approximately 1 to 1.5 L of simulant was added to a vessel, located at the bottom of the column, for each experiment. Each vessel was equipped with a water jacket, which circulated warm water to maintain the temperature at 45 ± 2 °C. Each column also has several ports, which were used to insert thermocouples and ER probes. Coupons were suspended from a rod with stainless steel rings at four different levels and exposed to the GW simulant and column vapor space. These levels are described as follows.

Immersed: Coupons are suspended in the vessel simulant for the whole duration of the test (i.e., 6 months). This represents continuous contact between the secondary liner and the groundwater.

Level 1: Bottom or low level. Coupons were dipped in the simulant for five minutes prior to testing. The coupons were hung at the bottom fixed ring of the rod shown in Figure 5-16 (b). These coupons were suspended approximately 1 inch above the liquid level of the simulant. Every two weeks, the coupons were lowered into the simulant for 5 minutes. This level is representative of the secondary liner bottom plate experiencing periodic wetting/drying.

Level 2: Intermediate or middle level. Coupons were dipped in the simulant for five minutes prior to testing. The coupons were hung at the middle-fixed ring approximately 18 inches above the liquid simulant in each vessel. This level is representative of a vapor space region of the secondary liner bottom that at one time was exposed to water, but since then has had infrequent or no contact with water. However, this region is exposed to the humidified air that may re-dissolve soluble salts that exist on the metal surface.

Level 3: Top or high level. This set of coupons was not exposed to the solution prior to testing. The coupons were suspended approximately 36 inches above the simulant. This level is representative of the secondary liner bottom plate region that is only exposed to the humidified air and any volatile species from the solution.

(a) **(b)**

Figure 5-16 Images of the (a) experimental configuration, and (b) steel rod to suspend the coupons

Table 5-10 lists the vessel, the corresponding VCI strategy, coupon configuration, number of coupons, and the coupon removal interval. Vessel 1 contained the GW simulant alone. Twenty-four base coupons, six at each level were utilized for this control test. No VCI was added to this vessel during the test in order to evaluate if the corrosion rate decreases with time during a 6-month test, perhaps due to the presence of a corrosion product. This test effectively provided a control for the previous testing with VCIs.

For Vessel 2, initially the twenty-four base coupons, six at each level, were exposed to GW simulant alone for 2 months. Twelve of these coupons were removed to establish the corrosion rate for carbon steel in an uninhibited environment. At that point in the test, 25% of the recommended dosage of VCI-B was injected into the vessel. The remaining 12 coupons were exposed to the VCI for an additional 4 months. Thus, the VCI's effectiveness at inhibiting a corroding surface could be evaluated.

For Vessel 3, twelve modified coupons, 3 at each level, were exposed to GW simulant plus 100% of the recommended dosage of VCI-B for 6 months. The potential of each sample was monitored periodically. The hypothesis for this test that as the VCI migrated up the column the potential measured at the surface would change once the inhibitor contacted the carbon steel surface. Thus, the migration time for the VCI could be estimated based on the time that was needed for the potential at the surface to change.

For Vessel 4, two modified coupons were immersed in the GW simulant alone for 6 months. The results of this test would provide a baseline potential that could be compared with the potentials measured in Vessel 3.

Table 5-10 Experimental details of Vapor Space Corrosion Setup

Vessel	VCI strategy	Coupons (configuration/number)	Frequency of coupons' removal (months)
1	GW only (Control)	Base/24	6
2	GW + 25% of recommended dosage VCI-B	Base/24	2 and 6
3	GW + 100% of recommended dosage VCI-B (potential measurements)	Modified/12	6
4	GW only (potential measurements)	Modified/2	6

5.4 Coupling Current Tests

Coupling current experiments were conducted to determine the effect of partial coverage of the DST bottom floor if VCIs are delivered through the leak detection pit. The partial coverage is defined when VCI is not fully delivered throughout the bottom surface. A series of experiments, listed in the following table, were conducted. The experiments involved two electrolytes in separate beakers, and the two beakers electrolytically interconnected by a salt bridge. The electrolytes, approximately 200 ml, were either the GW simulant or the GW simulant dosed with VCI-B at various levels. One carbon steel coupon was placed in each beaker, and the coupling current was measured between the coupons utilizing the potentiostat as a zero-resistance ammeter (ZRA). If large currents are detected, there is a possibility that accelerated corrosion may occur in areas with partial coverage.

Table 5-11. Matrix for Coupling Current Tests

Experiment No.	Electrolytes
1	Two carbon steel coupons in a beaker filled with GW simulant
2	Electrolytes 1 and 2 being the GW simulant
3	Electrolyte 1: GW simulant dosed with 100% VCI-B, Electrolyte 2: GW simulant
4	Electrolyte 1: GW simulant dosed with 100% VCI-B, Electrolyte 2: GW simulant dosed with 50% VCI-B
5	Electrolyte 1: GW simulant dosed with 100% VCI-B, Electrolyte 2: GW simulant dosed with 25% VCI-B
6	Electrolyte 1: GW simulant dosed with 50% VCI-B, Electrolyte 2: GW simulant dosed with 25% VCI-B
7	Electrolyte 1: GW simulant dosed with 50% VCI-B, Electrolyte 2: GW simulant
8	Electrolyte 1: GW simulant dosed with 25% VCI-B, Electrolyte 2: GW simulant

5.5 Quality Assurance

Data for all Tasks were recorded in the electronic laboratory notebook system, notebook number G8519-00126-14, J1719-00476-03 and, J1719-00476-04.

Requirements for performing reviews of technical reports and the extent of review are established in manual E7 2.60. SRNL documents the extent and type of review using the SRNL Technical Report Design Checklist contained in WSRC-IM-2002-00011, Rev. 2.

6.0 Results and Discussion

The results and discussion for the report are enumerated by the corresponding task.

6.1 Underdeposit Corrosion Testing

The experiments were conducted with coupons exposed to baked and as-prepared sludge as was described in Section 5. The coupons of the six experiments, listed in Table 5-7, were exposed for various durations as listed in Table 6-1. The coupons in Experiments 1 and 2 were exposed for 2502 hours. The Experiment 3 coupon was exposed for 1057 hours (Note: this experiment was stopped early due to heat-induced breakage of the experimental glass vessel). The Experiment 4 coupon was exposed for 2017 hours. The Experiment 5 and 6 coupons were exposed for 2981 hours.

The OCP data for coupons 1 and 2 are presented in Figure 6-1. Initially, during the first 500 hours, the potentials for both coupons decreased from approximately -200 mv vs. SCE to values between -350 to -400 mV vs. SCE. Between 500 to 1500 hours, the potential increased to values between -300 to -350 mV vs. SCE, where it remained at relatively constant values for the remainder of the test. The steady OCP value for the completely covered sample was approximately 40 mV less than that measured for the partially covered sample.

EIS scans were also collected at various instances during the coupon exposures. The EIS data in form of Bode plots for Coupons 1 and 2 are presented in Figure 6-2, and EIS data phase angles versus frequency is presented in Figure 6-3. The change in the ohmic resistance with time is observed by examining the high frequency (i.e., greater than 100 Hz) range of the Bode plot in Figure 6-2. A 3- to 5- fold increase in the ohmic resistance with time was seen over the 3 months that the tests were monitored. Most of this change occurred after the first month, after which the resistance remained at a steady value. In this case, the ohmic resistance for the complete coverage surface was greater than the partial coverage surface.

The OCP data for coupons 3 and 4 are presented in Figure 6-4. Initially, during the first 150-200 hours, the potentials for both coupons decreased from approximately -175 mv vs. SCE to values between -350 to -400 mV vs. SCE. For coupon 3, the completely covered surface, the potential increased to values between -250 to -300 mV vs. SCE for the time period from 200 hours to 1100 hours. At this time, the potential appeared to be stabilizing at -275 mV vs. SCE. However, this was the last reading that was taken due to an issue with a cracked glass vessel. For coupon 4, the potential increased to values between -200 to -250 mV vs. SCE for the time period between 150 hours to 700 hours. After 1800 hours the OCP appears to be approaching a steady value of -240 mV vs. SCE. Although it is difficult to make a complete comparison due to the duration of the coupon 3 test, the steady OCP value for the completely covered sample was approximately 35 mV less than that measured for the partially covered sample. This difference is similar to what was observed for coupons 1 and 2. It was observed that the OCP values for coupons 3 and 4 were greater than that observed for coupons 1 and 2. The corroded oxide surface may explain this difference.

EIS scans were also collected at various instances during the coupon exposures. Coupon 3 EIS data in form of Bode plot and phase angle versus frequency are presented in Figure 6-5 and Figure 6-6, respectively. Similarly, the Coupon 4 EIS data in form of Bode plot and Phase versus frequency are presented in Figure 6-7 and Figure 6-8, respectively. A 3-to 8- fold increase in the ohmic resistance with time was seen over the 1-2 months that the tests were monitored. Most of this change occurred after the first month, after which the resistance remained at a steady value. In this instance, the ohmic resistance for the partial coverage surface was greater than the complete coverage surface. It is not completely known whether the difference in exposure time or the difference between a corroded and a non-corroded surface resulted in a change.

However, the ohmic resistance for the partially covered samples (i.e., coupons 2 and 4) have very similar values.

The OCP data for Coupons 5 and 6 are presented in Figure 6-9. Initially, the OCP for both coupons were between -375 to -400 mV. The OCP in this case gradually increases with time for both coupons to values between -200 to -250 mV after 2000 hours. The increase in OCP likely reflects the difference in sludge layer adherence. After that time, the OCP values are relatively stable. At test completion, the OCP for the completely covered sample was approximately 40 mV less than that for the partially covered sample. This difference was consistent for all three sets of tests. Additionally, the final steady OCP values for all pairs of coupons were very similar.

EIS scans were also collected at various instances during the coupon exposures. The EIS data in form of Bode plots for the Coupons 5 and 6 are in Figure 6-10 and phase angle versus frequency is presented in Figure 6-11. A 3- 5- fold increase in the ohmic resistance with time was seen over the 2.5 months that the tests were monitored. Most of this change occurred after the first month, after which the resistance remained at a steady value. In this instance, the ohmic resistance for the complete coverage surface was greater than the partial coverage surface. Additionally, it was observed that the final ohmic resistance for all pairs of coupons was very similar.

Table 6-1 Exposure Duration

Experiment	Deposit Condition	Duration (hours)
1	Adherent AZ-101 baked-sludge deposit completely covering the coupon	2502
2	Adherent AZ-101 baked-sludge deposit partially covering the coupon	2502
3	Adherent AZ-101 baked-sludge deposit completely covering the coupon	1057
4	Adherent AZ-101 baked-sludge deposit partially covering the coupon	2071
5	AZ-101 as-prepared sludge completely covering the coupon (Control)	2981
6	AZ-101 as-prepared partially covering the coupon (Control)	2981

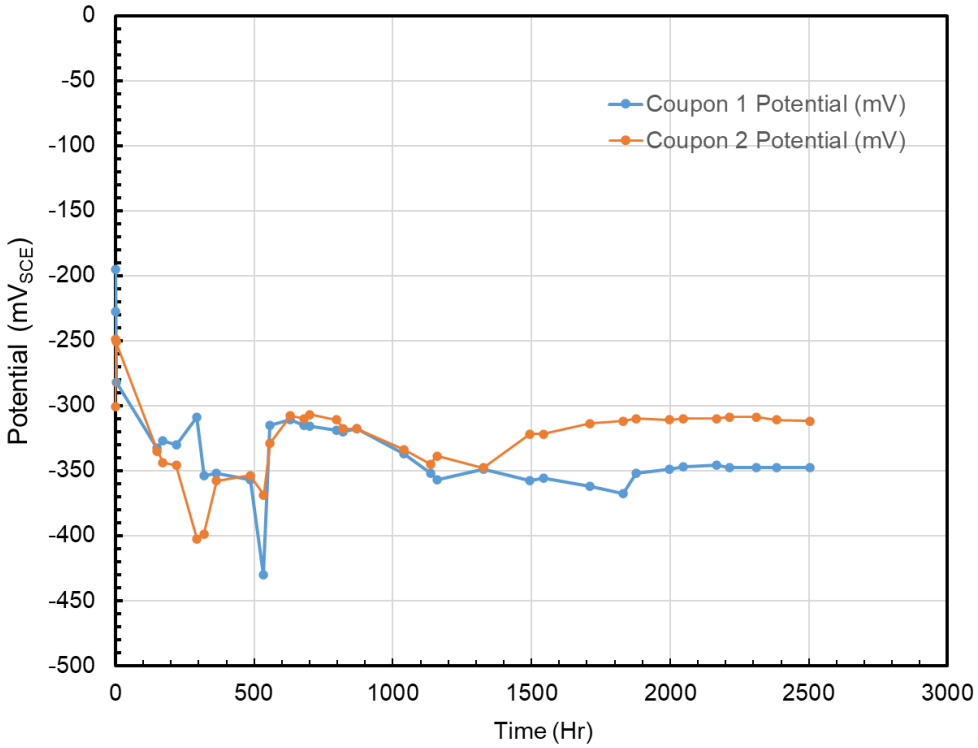

Figure 6-1. Coupons 1 (baked sludge, complete coverage) and 2 (baked sludge, partial coverage) OCPs

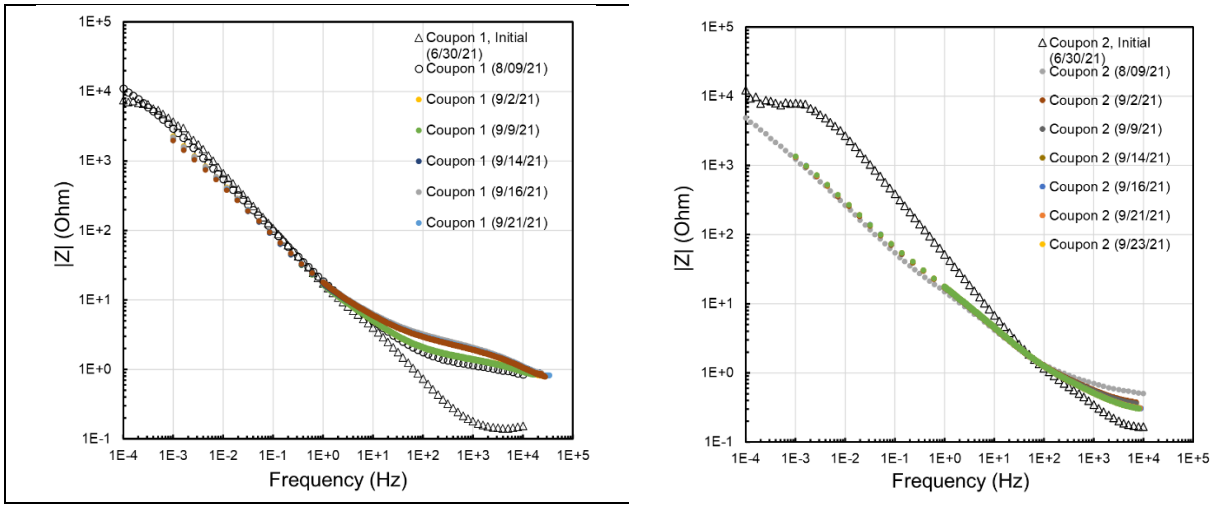

Figure 6-2. Coupons 1 and 2 EIS Data, Bode Plot

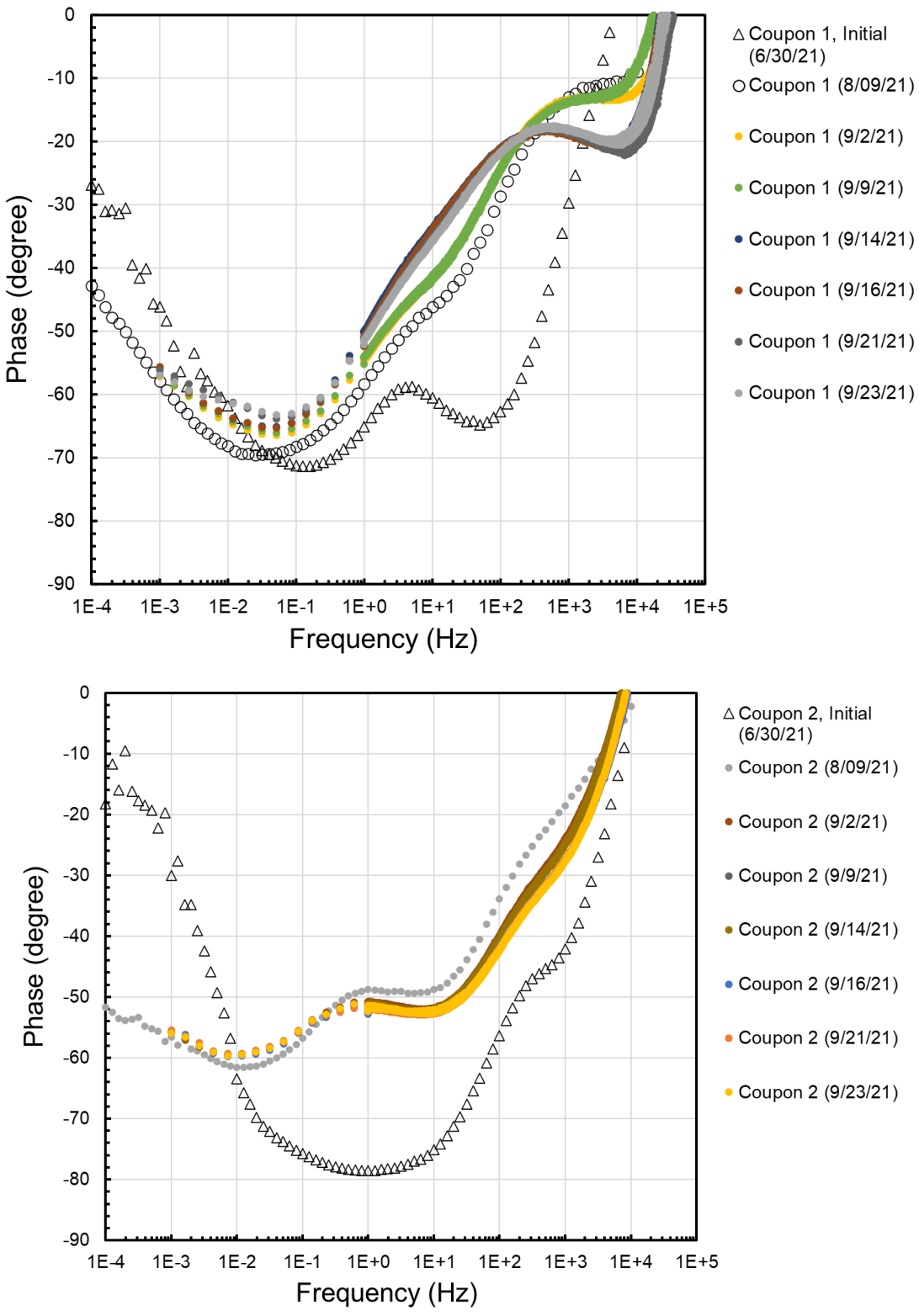

Figure 6-3. Coupons 1 and 2 EIS Data, Phase vs. Frequency

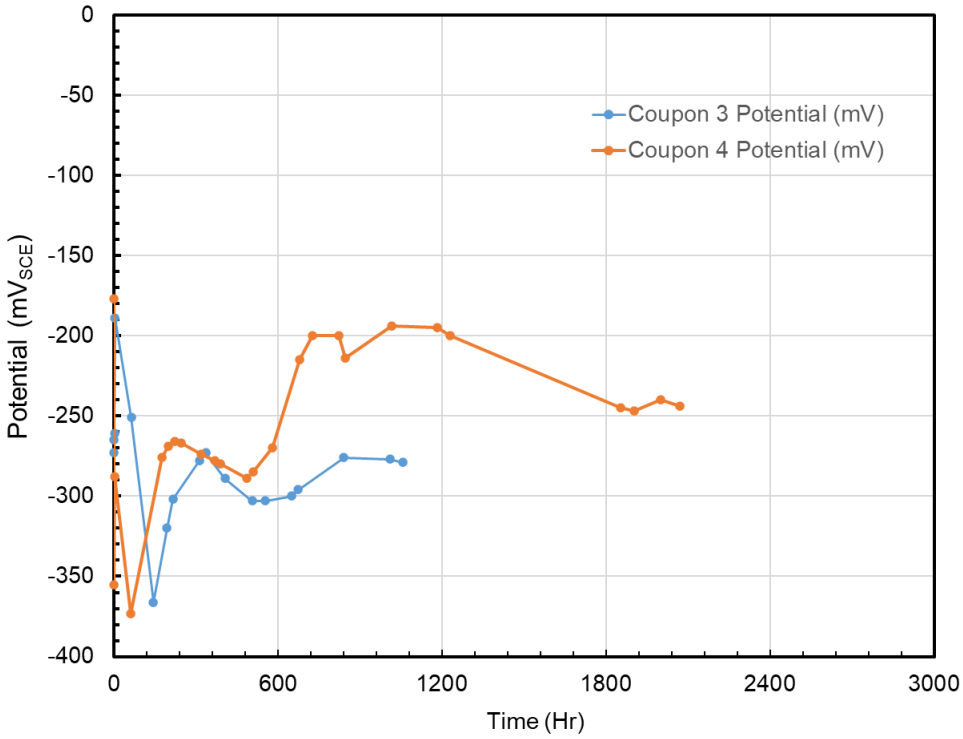

Figure 6-4. Coupons 3 (baked sludge layer, complete coverage) and 4 (baked sludge layer, partial coverage) OCPs. Both Coupons 3 and 4 were pre-corroded in GW simulant for two months before start of the underdeposit tests.

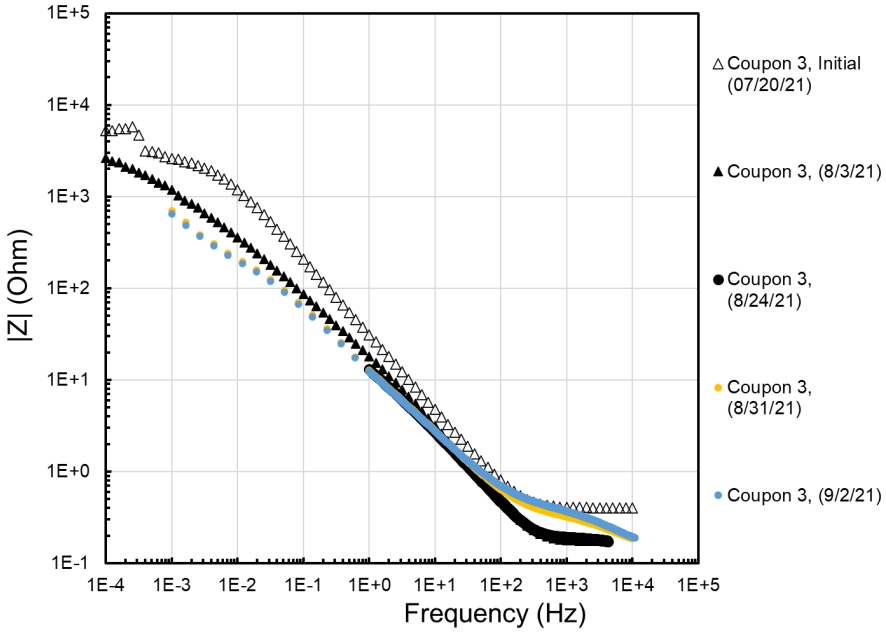

Figure 6-5. Coupon 3 EIS Data, Bode Plot

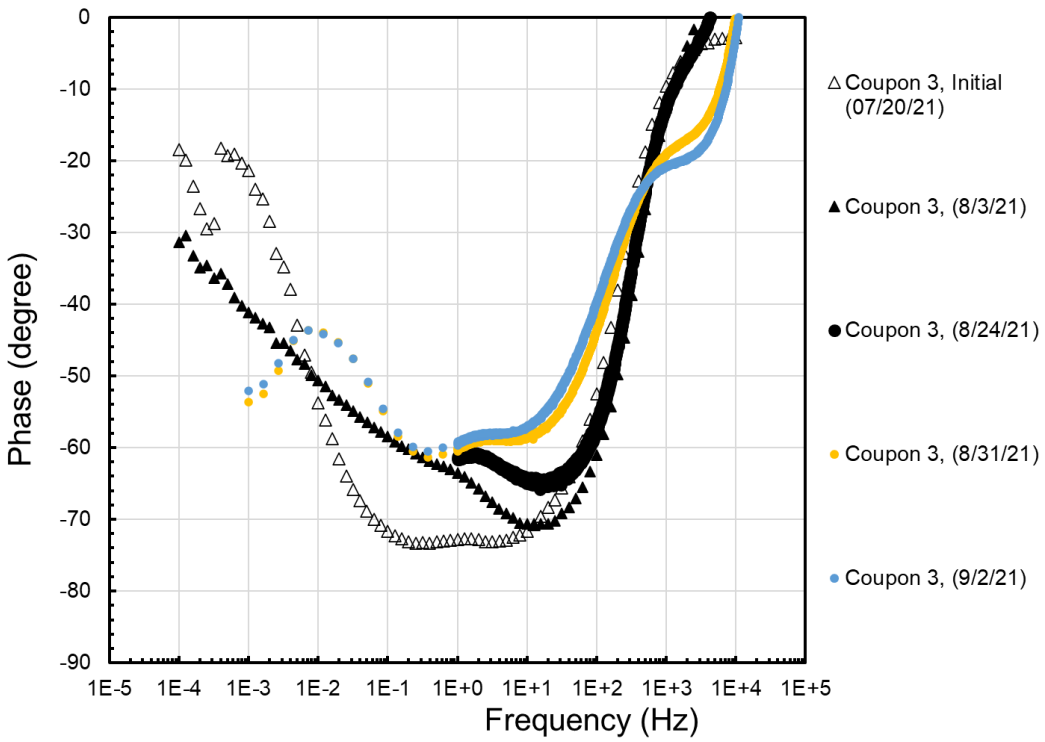

Figure 6-6. Coupon 3 EIS Data, Phase vs. Frequency

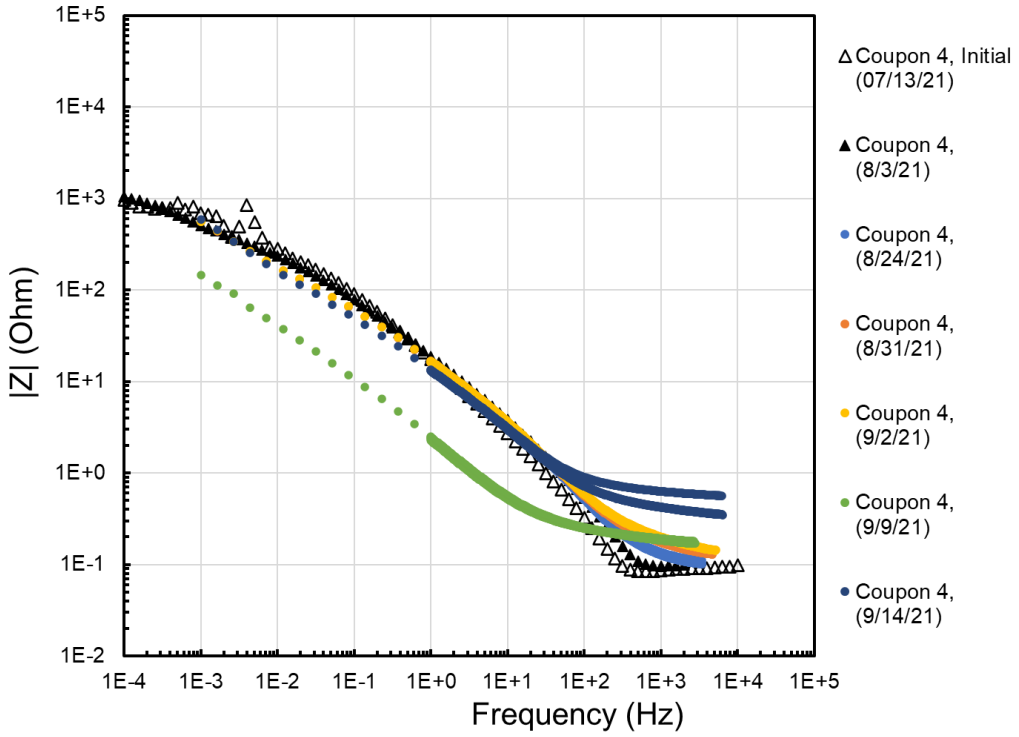

Figure 6-7. Coupon 4 EIS Data, Bode Plot

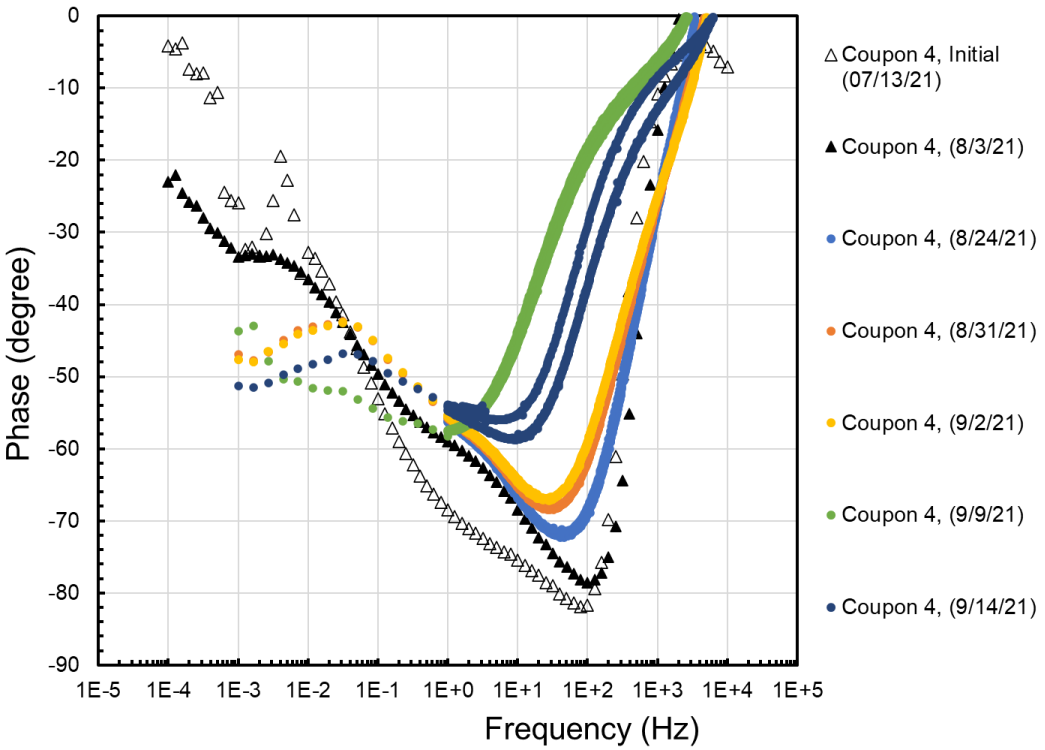

Figure 6-8. Coupon 4 EIS Data, Phase vs. Frequency

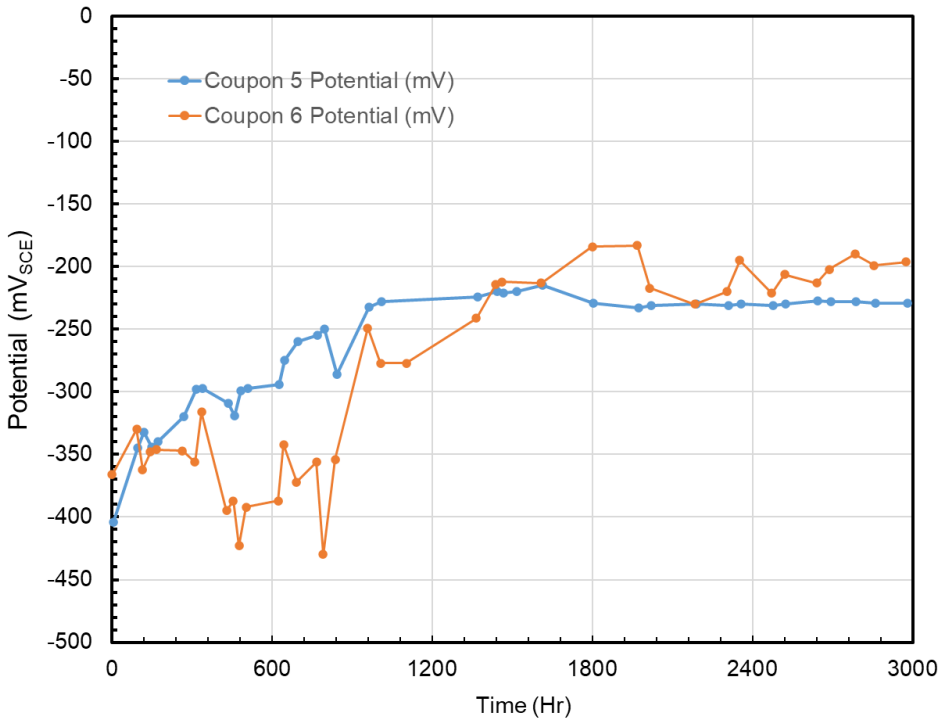

Figure 6-9. Coupons 5 (as-prepared sludge, complete coverage) and 6 (as-prepared sludge, partial coverage) OCPs

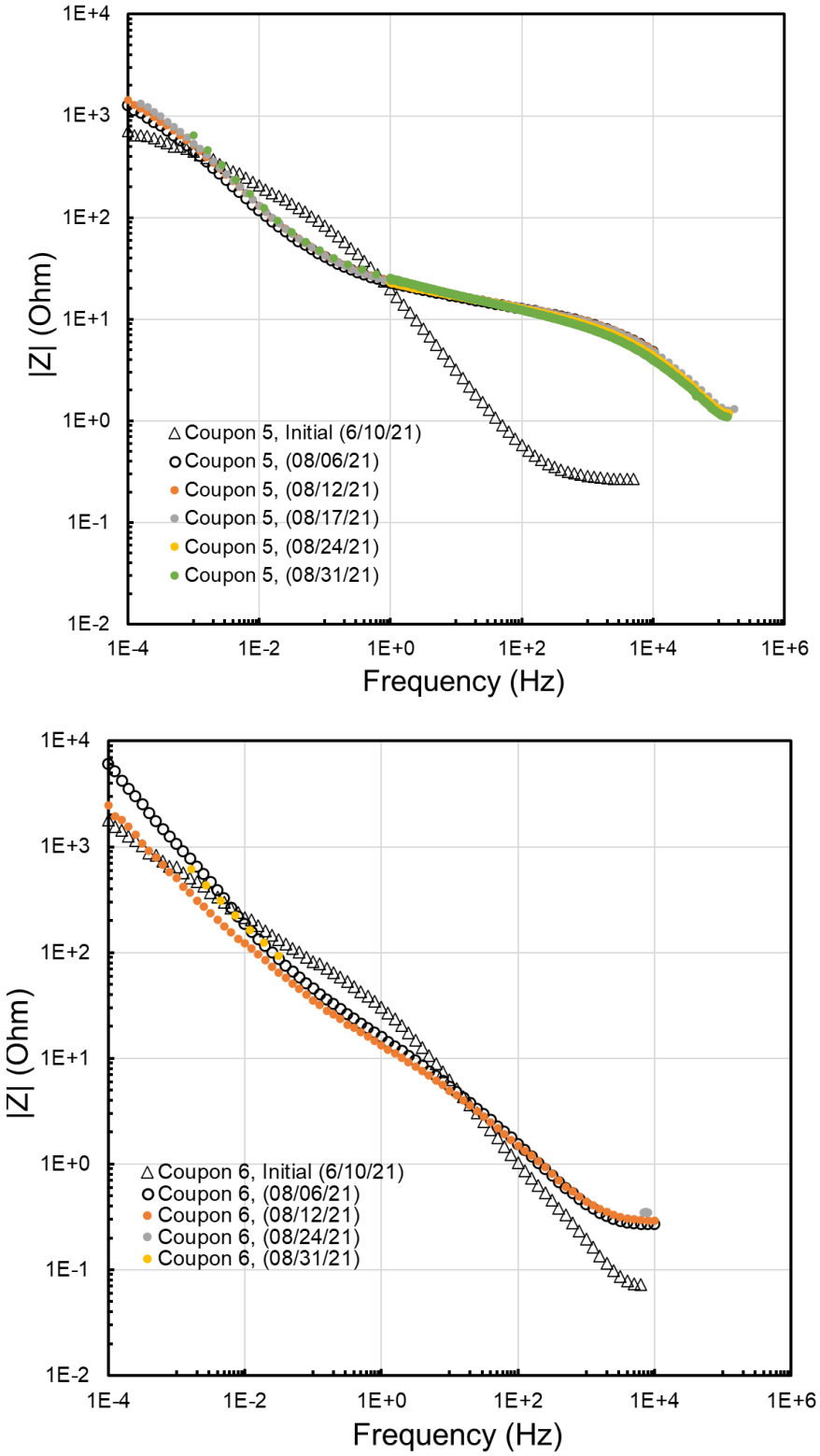

Figure 6-10. Coupons 5 and 6 EIS Data, Bode Plot

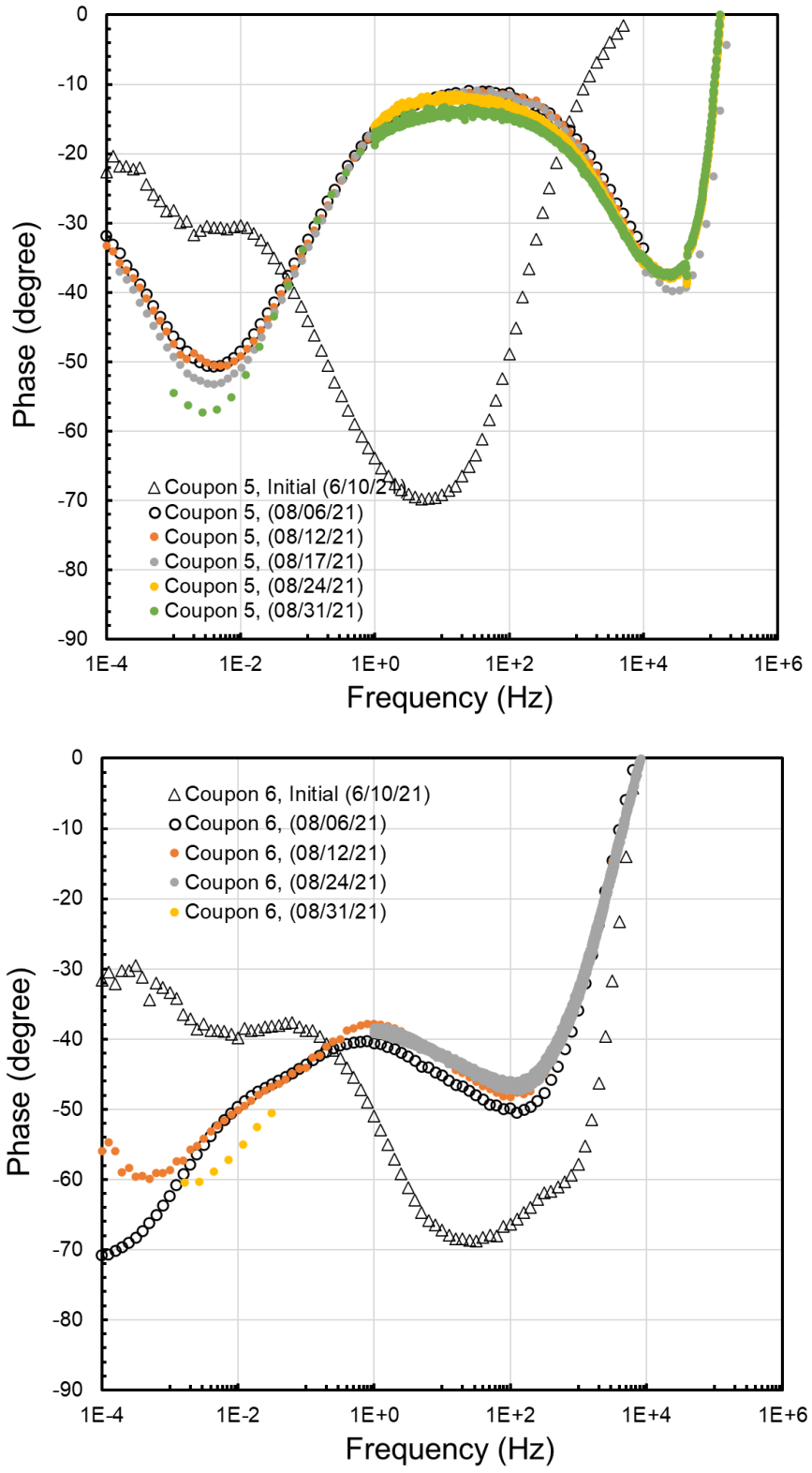

Figure 6-11. Coupon 5 and 6 EIS Data, Phase vs. Frequency

Figure 6-12 shows post-test images of each of the coupons. From a macroscopic viewpoint, there appeared to be little attack of the metal surface.

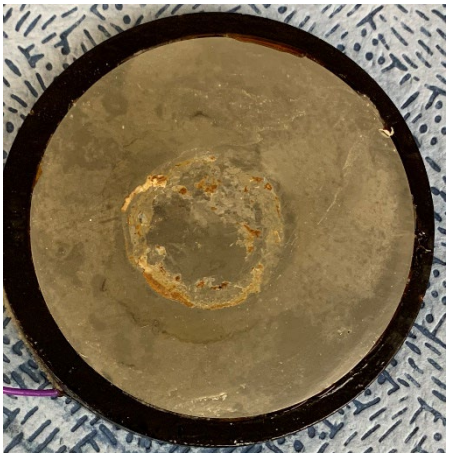

Experiment 2

Experiment 1

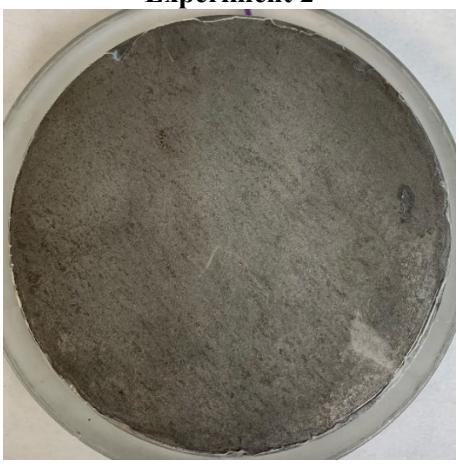

Experiment 4

Experiment 3

Experiment 5

Experiment 6

Figure 6-12. Post-test images of the coupons tested using the sludge deposits

A summary of the OCP and EIS data for each coupon is listed in Table 6-2.

Table 6-2. OCP and EIS Data Summary

Condition	Coupon	Data Values	
		OCP (mV_{SCE})	High Frequency EIS (Ohm) and Phase Angle
Baked Sludge	1 (entire coupon)	-348 (2502 hr)	• 0.14 Ω (initial, 6/30), -2.7 • 0.85 Ω (8/9), -9 (8/9) • 0.8 Ω (9/2), -0.5 (9/2) at 26 kHz • 0.84 Ω (9/9), -0.5 (9/9) at 16 kHz • 0.9 Ω (9/14), -0.4 (9/14) at 21.7 kHz
	2 (partially covering)	-312 (2502 hr)	• 0.17 Ω (initial, 7/13), -9 • 0.5 Ω (8/3), -2.2 (8/3) • 0.37 Ω (9/2), -0.3 (9/2) at 7 kHz • 0.36 Ω (9/9), -0.02 (9/9) at 7.16 kHz • 0.31 Ω (9/14), -0.1 (9/14) at 7.5 kHz
Baked Sludge on pre-corroded coupons	3 (entire coupon)	-280 (1057 hr)	• 0.45 Ω (initial, 7/30), -2.9 • 0.17 Ω (8/3), -1.7 (8/3) • 0.18 Ω (8/24), -0.2 (8/24) at 4.22 kHz • 0.19 Ω (8/31), -0.3 (8/31) at 9.67 kHz • 0.19 Ω (9/2), -0.3 (9/2) at 9.67 kHz
	4 (partially covering)	-244 (2071 hr)	• 0.1 Ω (initial, 7/13), -7 • 0.1 Ω (8/3), -4.9 (8/3) • 0.1 Ω (8/24), -0.1 (8/24) at 3.43 kHz • 0.12 Ω (8/31), -0.3 (8/31) at 4.62 kHz • 0.14 Ω (9/2), -0.3 (9/2) at 5.19 kHz • 0.18 Ω (9/9), -0.03 (9/9) at 2.54 kHz • 0.35-0.56 Ω (9/14), -0.2 (9/14) at 6.24 kHz
Non-baked sludge (control)	5(entire coupon)	-229 (2981 hr)	• 0.267 Ω (initial), -1.5 • 4.82 Ω (8/6), -33.7 (8/6) • 4.93 Ω (8/12), -35.3 (8/12) • 1.30 Ω (8/17), -4.36 (8/17) at 173 kHz • 1.20 Ω (8/24), -0.2 (8/24) at 140 kHz • 1.10 Ω (8/31), -1.26 (8/31) at 134 kHz
	6 (partially covering)	-196 (2981 hr)	• 0.072 Ω (initial), -4.2 • 0.272 Ω (8/6), -1.71 (8/6) • 0.293 Ω (8/12), -3.34 (8/12) • 0.35 Ω (8/25), -0.3 (8/24) at 8 kHz • 0.37 Ω (8/31), -0.1 (8/31) at 7.3 kHz

The coupons were profiled using laser-based and visible-light-based profilometers. Coupon 1 profiled images are presented in Figure 6-13; few minor pits were noticed throughout the coupon surface, with the

deepest pit being ~80 µm deep. The profiled image of Coupon 2 is presented in Figure 6-14. Similar to Coupon 1, small pits were noticed throughout the coupon surface, with the deepest pit being ~70 µm deep.

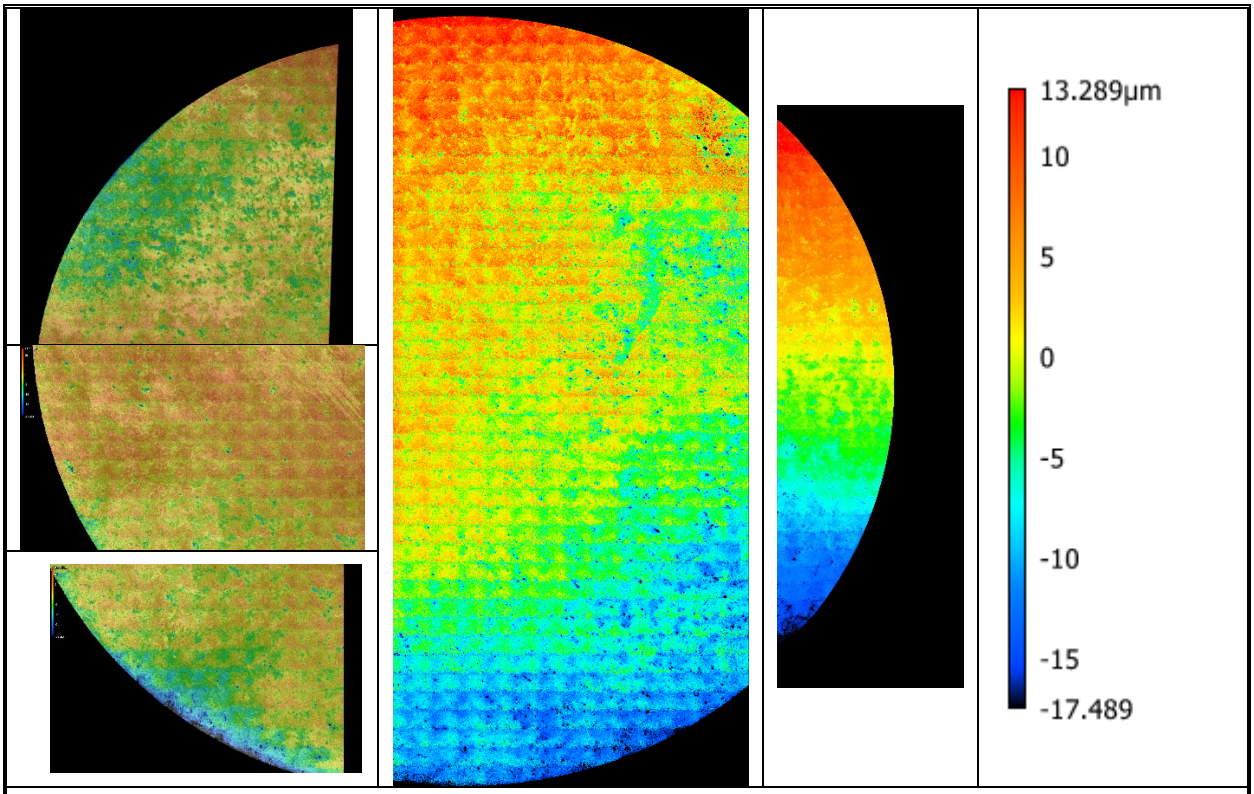

Figure 6-13. Profiled image of Coupon 1.

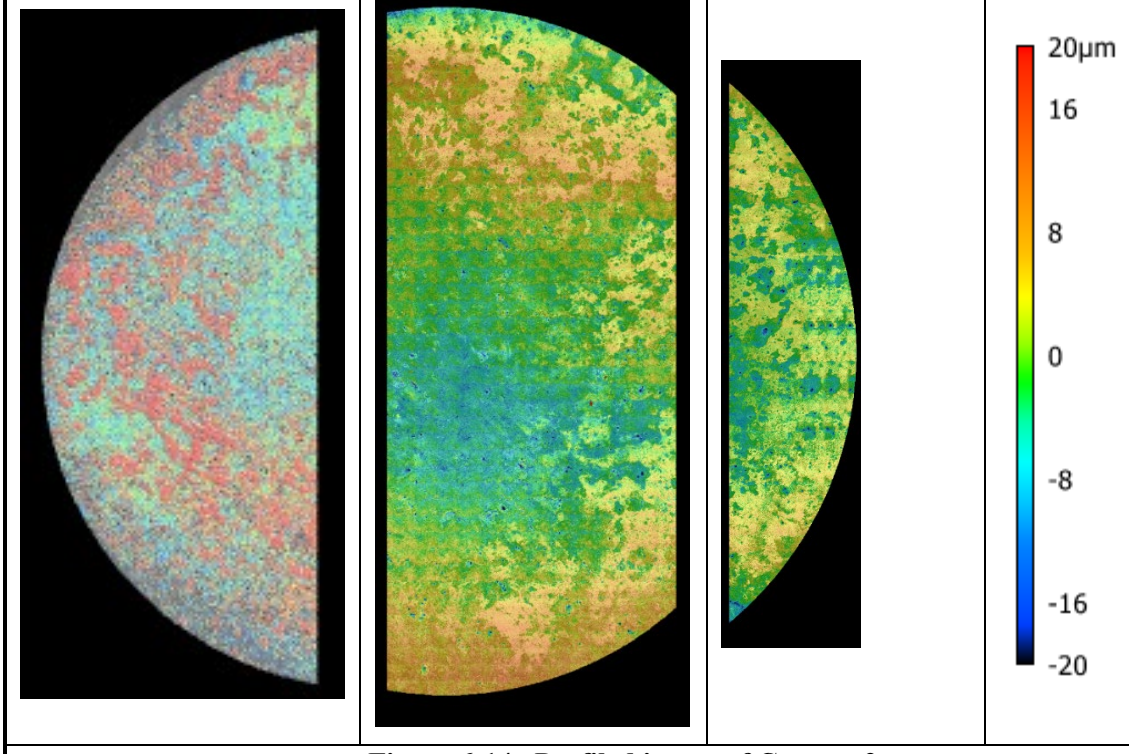

Figure 6-14. Profiled image of Coupon 2.

Profiled images of Coupons 3, 4, 5, and 6 are presented in Figure 6-15, Figure 6-16, Figure 6-17, and Figure 6-18, respectively. A summary of the coupons' profiles images and coupons' corrosion rates are listed in Table 6-3.

An analysis of the OCP and EIS data, coupled with micropit observations, and mass-loss based corrosion rate data provide following insights:

- The baked sludge resistivity evolved over-time, as noted in the high-frequency impedance data. However, the final ohmic resistance for all coupons were very similar after approximately 1 month of exposure. This indicated that the baked sludge is not stable in presence of the supernate. In the waste storage tanks, there is several feet of sludge layer beneath the supernate layer. The hydrostatic force of the supernate and sludge create a condition where the sludge layer in contact with the tank bottom experiences the weight above it; this creates a relatively drier sludge in contact with the waste tank. In the laboratory experiments, the hydrostatic force was much less, and therefore, the supernate was able to percolate, and therefore, the baked sludge was not stable.

- The micropits that were observed in Coupons 1-4 may have initiated and grown when the baked sludge layer persisted at the coupon surface. The initial decrease in the potential with time, may indicate this occurred. However, as the baked sludge layer became imbued with the supernate and the resulting became similar to the as-prepared sludge, pit growth ceased. The increase in potential during the later stages indicates that this may have occurred.

- In contrast, coupons 5 and 6 did not exhibit pitting. The OCP for these coupons increased from the time of exposure. This behavior suggests the formation of a passive oxide film.

Table 6-3 Underdeposit Coupon Summary

Experiment	Data Values		
	Micropit presence and exposure duration	**Deepest Pit (µm)**	**General Corrosion Rate (mpy)**
1	Throughout coupon surface (2502 hr)	~80 µm	0.26
2	Throughout coupon surface (2502 hr)	~70 µm	0.26
3	Very few (1057 hr)	~83 µm	0.21
4	Very few (2071 hr)	~58 µm	0.34
5	None (2981 hr)	Not applicable	0.52
6	None (2981 hr)	Not applicable	0.51

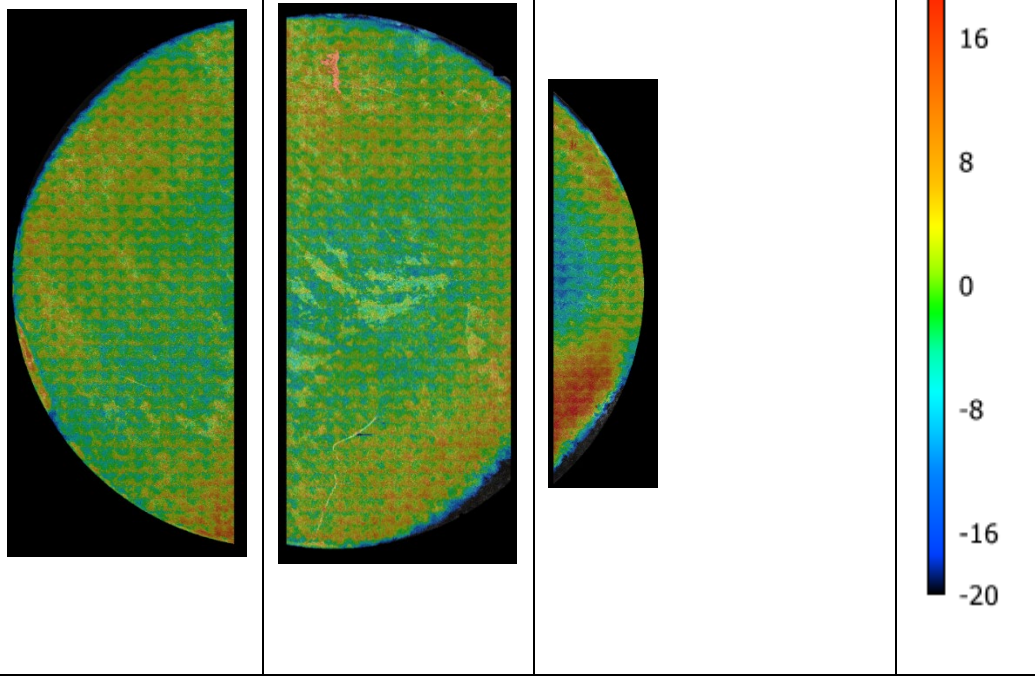

Figure 6-15. Profiled image of Coupon 3.

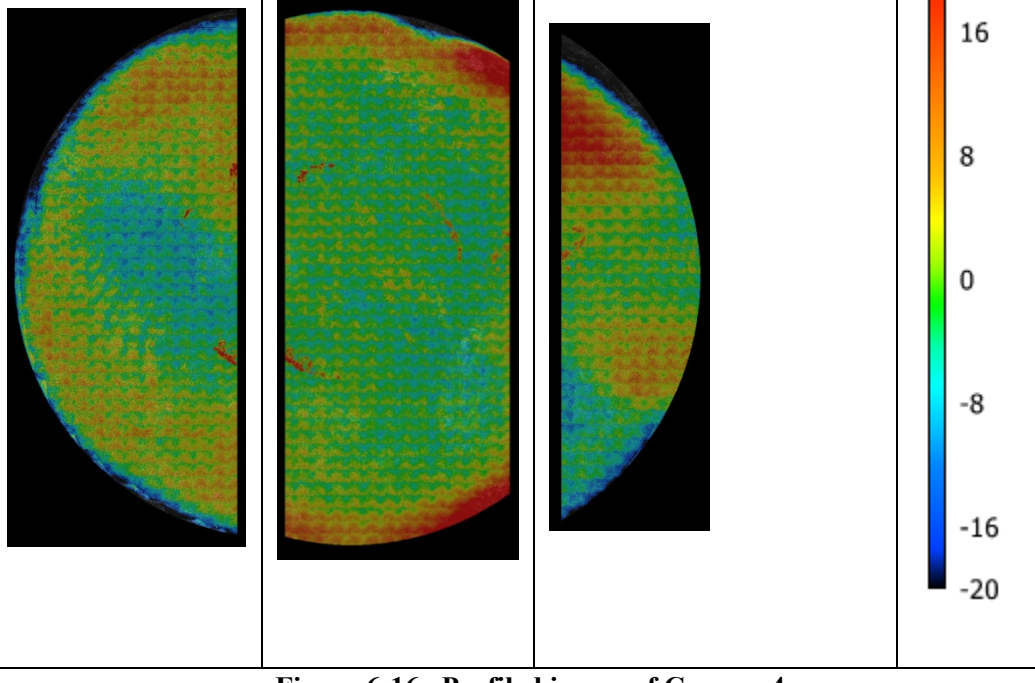

Figure 6-16. Profiled image of Coupon 4.

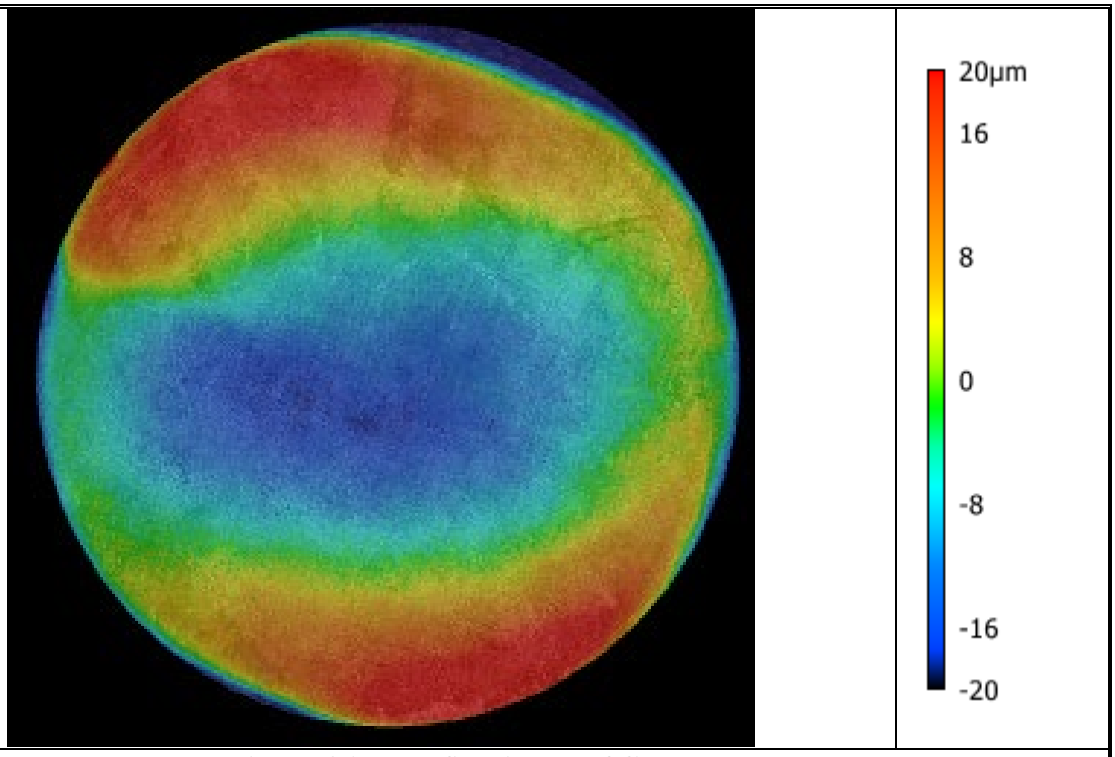

Figure 6-17. Profiled image of Coupon 5.

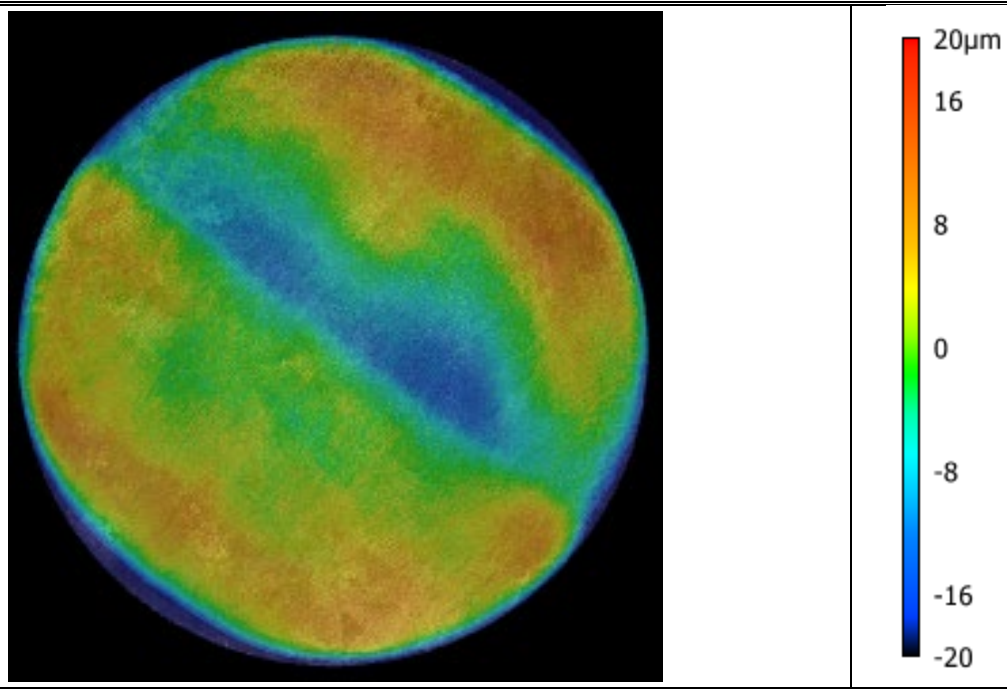

Figure 6-18. Profiled image of Coupon 6.

6.2 Secondary Liner Corrosion

6.2.1 Control Test with Groundwater Solution

A control test with the GW simulant was conducted for a duration of six months. The test was conducted to determine if the corrosion rate begins to decrease after the 2-month exposure or if the rate stays steady for the 6-month duration of the test. Furthermore, if the corrosion rate does decrease, is it similar to the decrease in corrosion rate that was observed after the addition of VCI? To this end, the two-month data collected during FY19 and FY20 studies are compared to the six-month data collected during FY21 study; the data are listed in Table 6-4 and is graphically presented in Figure 6-19. In addition, the corrosion rate data for the VCI-treated GW simulant is also included in Table 6-4.

Table 6-4. Mass-loss data of the coupons exposed for two- and six-months in the ground water simulant

Level	Coupon Mass Loss (mg)			
	2-month exposure**	**6-month exposure****	**6-month exposure with VCI-A*****	**6-month exposure with VCI-B******
Immersed	90.7 ± 12.5	155.7 ± 17.0	120 ± 0.3	79.8 ± 10.1
Level 1	44.3 ± 26.3	130.3 ± 20.7	88.5 ± 26.8	44.9 ± 8.8
Level 2	57.7 ± 18.9	87.6 ± 13.6	71.2 ± 13.3	39.7 ± 5.4
Level 3	35.3 ± 13.8	126.9 ± 38.0	71.2 ± 18.7	35.5 ± 20

**2- and 6-month coupons were exposed to GW simulant only, each data point for 2-month corrosion rate represent average of 12 coupons and each data point for 6-month coupon represent average of six coupons. It is noted that the two-month data was collected in the GW simulants that were prepared in FY 19 and FY 20 whereas FY 21 data was collected in the simulant prepared in the same year; this may have introduced batch-to-batch variability that influenced the corrosion observed during the two-month period.

***6-month exposure with VCI-A data are for the coupons that were exposed to GW-only for initial two months and then exposed to GW + VCI-A for additional four months.

****6-month exposure with VCI-B data are for the coupons that were exposed to GW-only for initial two months and then exposed to GW + VCI-B for additional four months.

The data for the coupons exposed to GW simulant only for 2 and 6 months show that corrosion continues after two months of exposure, although the rate decreases slightly due the formation of corrosion product layers over the last 4 months. However, in the cases where VCIs were present for the last 4 months, an even more dramatic decrease in the corrosion rate was observed. For VCI-B, the observation that there is little difference between the mass loss after 6 months and the mass lost after 2 months is an indication that corrosion is effectively mitigated. The data highlight that VCIs can be an effective corrosion control measure to mitigate external corrosion of the secondary liner.

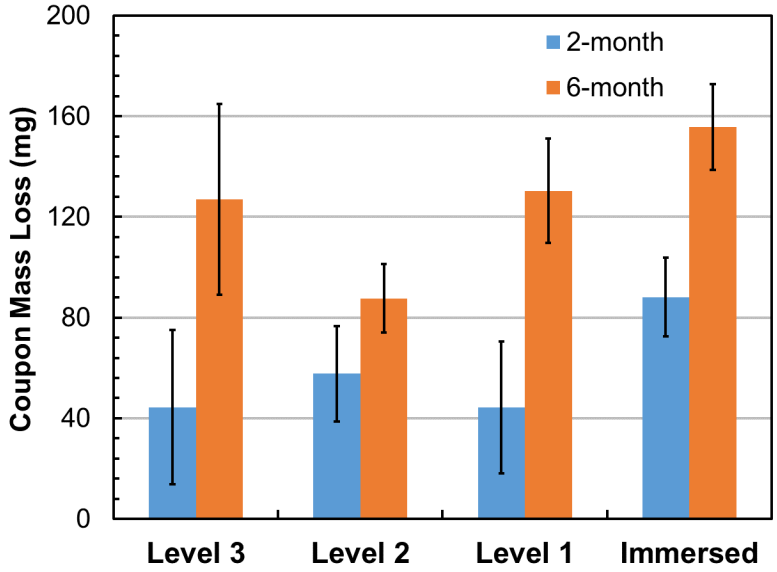

Figure 6-19. Two (blue) and six-month mass-loss data for coupons exposed to GW simulant only. The black line in each bar represents the standard deviation.

6.2.2 VCI Effect Experiment with 25% Concentration

In FY19 and FY20, VCI effect experiments were conducted with 100 and 50% of the VCI-B concentrations. It was determined that VCI-B is effective is mitigating corrosion at 50% or more of the recommended dosage. However, the threshold below which VCI-B ceases to be effective had not been determined. Therefore, an experiment was conducted at 25% of the recommended dosage of the VCI-B. The corrosion rate data is listed in Table 6-5; the surface average and deepest pit corrosion rate data are graphically presented in Figure 6-20. The profiled images of the two- and six-month coupons are presented in Figure 6-21 and Figure 6-22, respectively. The Student t-test p-values between two- and six-month coupons are listed in Table 6-6.

Table 6-5. Vessel 1 (25% VCI-B After Two Months) Coupon Corrosion Data

Corrosion Type	Corrosion Rate (mpy)*							
	Immersed		Level 1		Level 2		Level 3	
	2-month	6-month	2-month	6-month	2-month	6-month	2-month	6-Month
Surface Average Corrosion	6.17	2.39	0.70	1.81	4.32	1.32	2.40	1.77
	3.49	3.11	1.04	1.51	4.95	1.58	7.40	1.51
	5.11	2.33	0.63	1.37	4.86	1.98	1.63	1.90
Average** ± std***	4.92 ± 1.35	2.61 ± 0.44	0.79 ± 0.22	1.56 ± 0.23	4.71 ± 0.34	1.62 ± 0.33	3.81 ± 3.1	1.73 ± 0.2
Pitting Corrosion	27.1	24.4	13.9	17.2	34.8	12.2	42.9	11.1
	81.6	18.9	18.3	15.1	44.5	12.0	42.2	21.1
	30.4	18.9	9.7	19.7	32.9	15.4	16.5	16.6
Average** ± std***	46.4 ±30.6	20.8 ± 3.1	14.0 ± 4.3	17.3 ± 2.3	37.4 ± 6.2	13.2 ± 1.9	33.9 ± 15.1	16.2 ± 5.0

*25 μm/yr = 1 mil/yr = 1 mpy
**Average values are calculated for 3 coupons
***std denotes standard deviation of the corrosion rate data used to calculate the average

Table 6-6. Student T-test p-values between two- and six-month coupons

Level	Surface Average Corrosion Rate	Deepest Pit Corrosion Rate
Immersed	0.05	0.13
Level 1	0.01	0.003
Level 2	0.003	0.30
Level 3	0.31	0.22

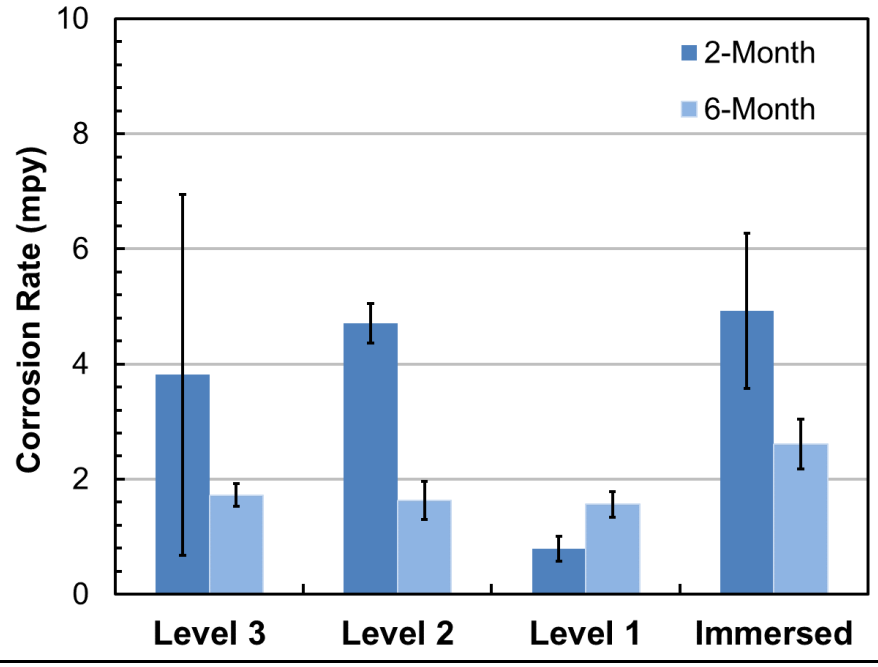

(a) Surface average corrosion rate

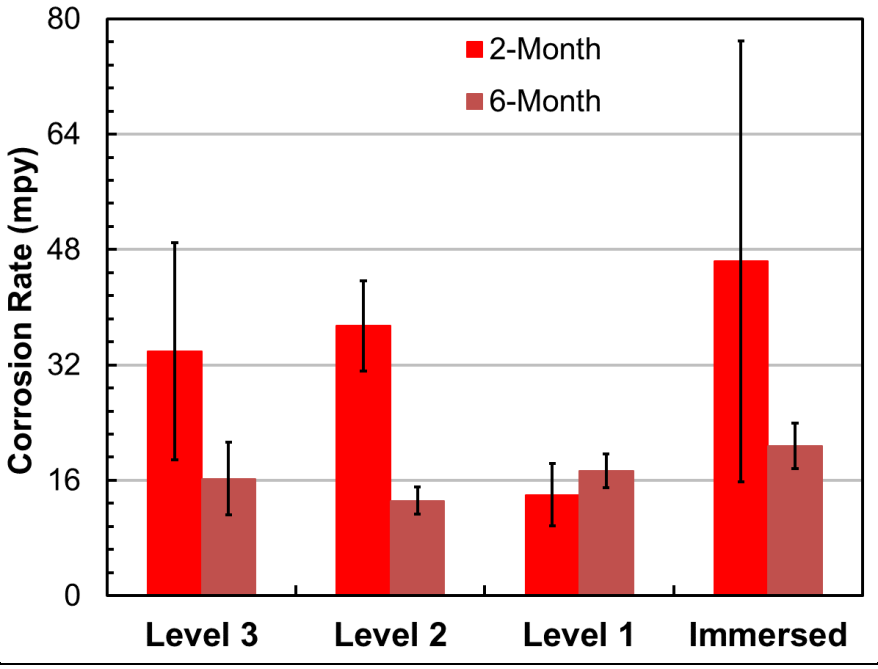

(b) Pitting corrosion rate

Figure 6-20. Average of (a) surface average, and (b) pitting corrosion rates for coupons in Vessel 1 (GW, and then GW +25% VCI-B). The black line in each bar represents the standard deviation.

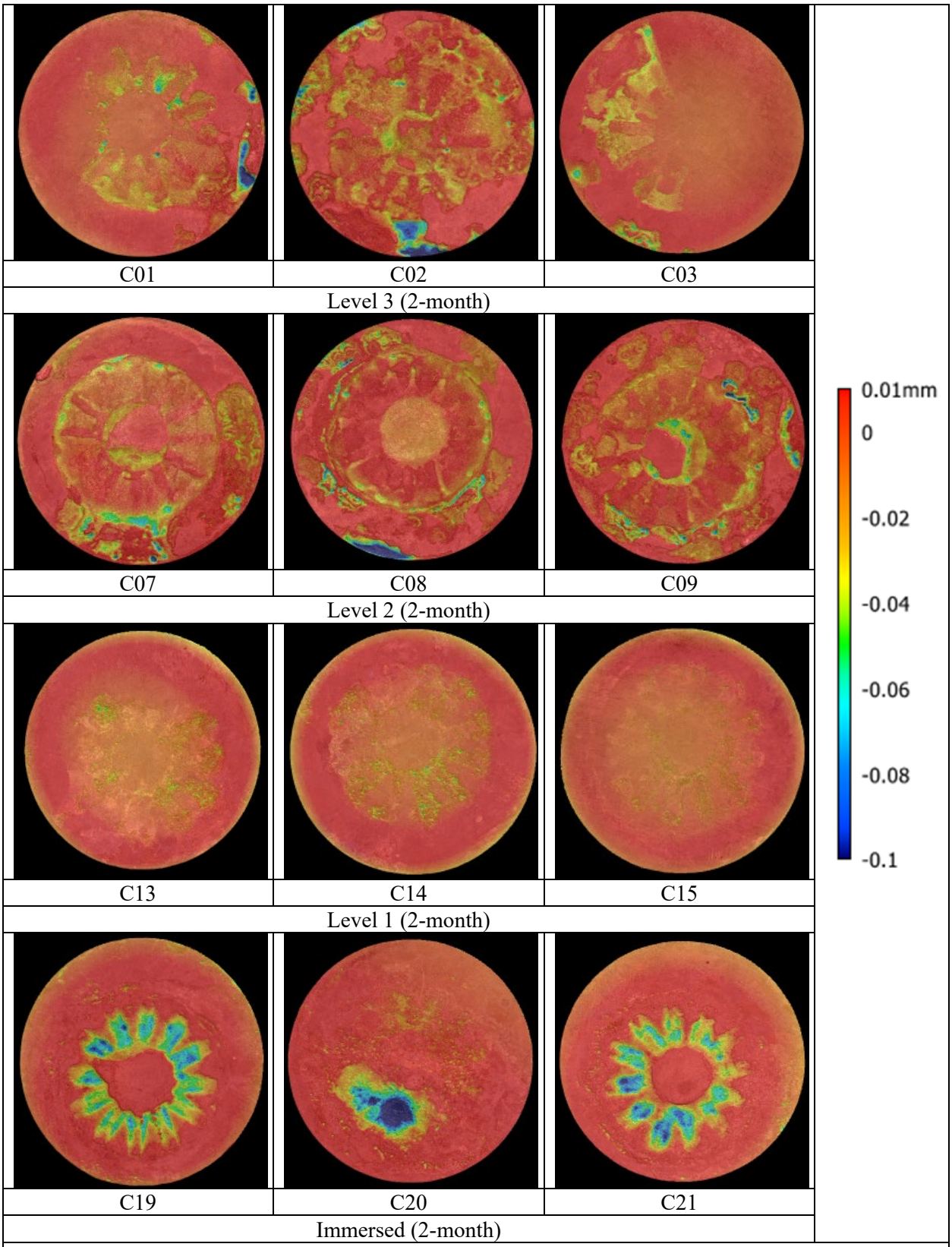

Figure 6-21. Profiled images of the coupons exposed for two-month in the GW + 25% VCI-B experiment.

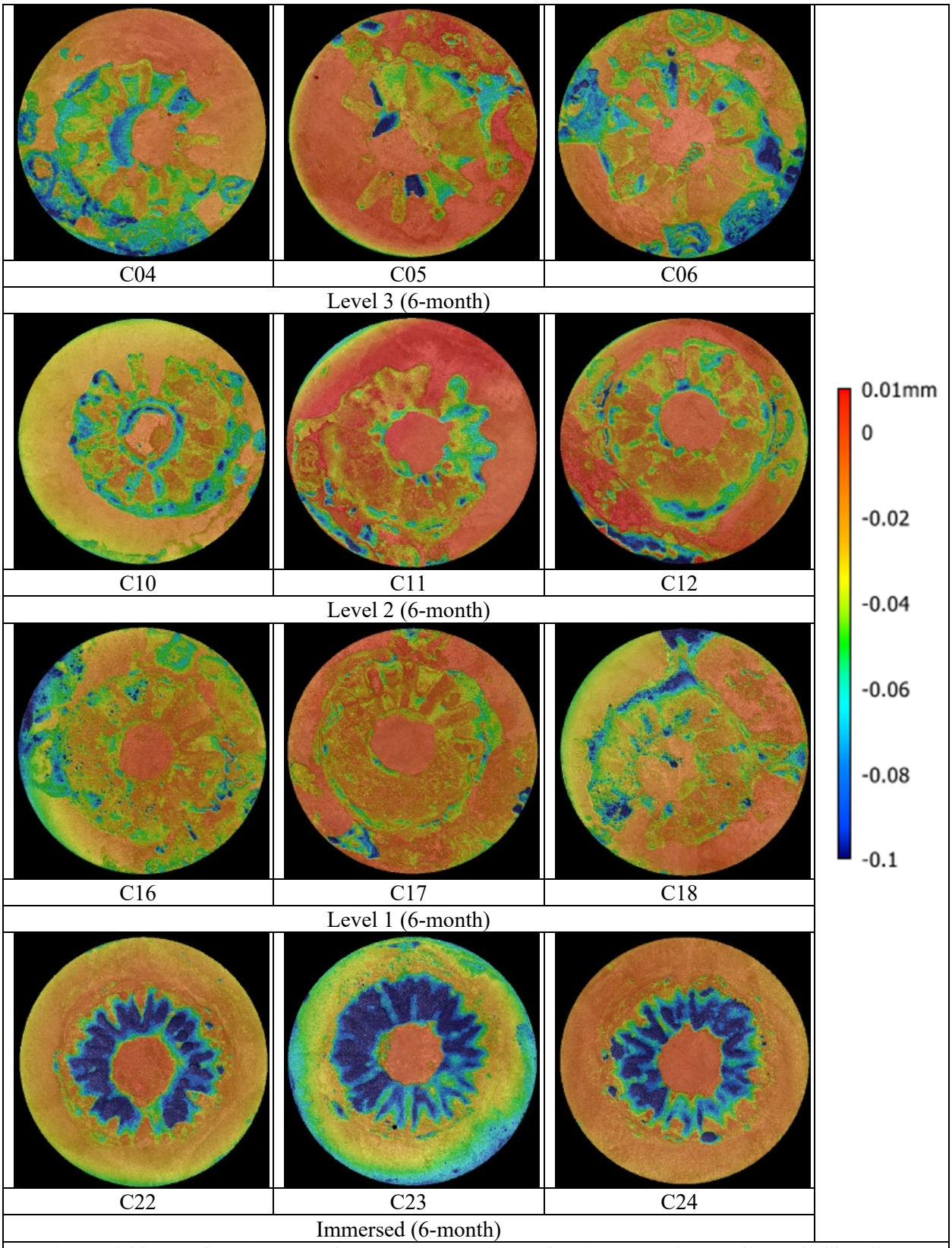

Figure 6-22. Profiled images of the coupons exposed for six month in the GW + 25% VCI-B experiment.

The Student's t-test p-values listed in Table 6-6 are based on the hypothesis that there is no statistically significant difference between the two- and six-month corrosion rates used in the t-test—that is, that they are essentially identical to each other in terms of the coupon corrosion rates. The statistical result calculated by the test, p-value, is the probability that the hypothesis is true. The higher the p-value, the greater the chance that the two sets of corrosion rates for the 2- and 6-month coupons are statistically similar. If the p-value is equal to or less than 0.05, it indicates that there is a less than 5% chance that the two sets of coupons have similar corrosion rates—that is, it means, with 95% confidence, that there is a statistically significant difference between the two 2- and 6-month coupons. The listed p-values in Table 5-6 show that 25% dosage of VCI-B was not sufficient to be able to mitigate surface average corrosion rates at Level 3, and mitigation at the immersed level is marginal. Similarly, the p-values for the deepest pit corrosion rates show that corrosion was not mitigated at immersed, and Levels 2 and 3. This result suggests that the threshold minimum dosage for VCI-B is between 25 and 50% of the recommended dosage. In practice, if the concentration of VCI-B decreased below 50%, it is likely that replenishment of the VCI would be necessary.

6.2.3 VCI Migration

The corrosion potentials of the "modified" coupons in Vessels 3and 4 were monitored periodically. The coupons were identified using a numerical value. The coupons identification numbers are listed in Table 6-7. The corrosion potentials of the coupons in immersed phase were measured with respect to the SCE and Pt-wire. The corrosion potential data for the coupons and Pt wires at immersed levels in Vessels 3 and 4 are presented in Figure 6-23. The corrosion potentials of the vapor space coupons could only be measured with respect to the Pt wire embedded in each coupon assembly; the data had considerable amount of scatter, which made drawing conclusions on the migrations of the VCIs challenging. The corrosion potential data are summarized in Table 6-8.

Table 6-7. Coupon identification numbers used to study VCI distribution

Level	GW simulant plus 100% VCI-B Experiment in Vessel 3	GW Simulant Only Experiment in Vessel 4
Immersed	34, 35, 36	37, 38
Level 1	31, 32, 33	—
Level 2	28, 29, 30	—
Level 3	25, 26, 27	—

The corrosion potentials of the immersed coupons in GW simulant are close to -325 mV_{SCE}, and in GW simulant + VCI were in the range of -50 to +50 mV_{SCE}. This indicated that corrosion potential difference is close to 300 mV between the GW simulant and GW simulant + VCI solutions. The corrosion potentials of the Pt wire in GW immersed solution are -300 and -50 $mV_{SCE,}$ and in GW simulant + VCI range between -100 to 200 mV_{SCE}; Pt wire potentials were not distinctly different and overlapped. A comparison between the SCE-measured and Pt-wire measured potentials indicated that Pt wire potentials are not stable, and a stable difference in the Pt wire potentials between the two solutions (GW simulant + VCI and GW simulant) was not established.

Table 6-8. Immersed Pt Wire and Coupons Potentials

Coupons/Pt Wire	Electrolyte	
	GW only	GW + 100% VCI-B
Pt wire (with immersed coupons) vs. SCE	Coupon 37 wire near -300 mV Coupon 38 wire near -50 mV	Coupons 34 and 36 wires near 200 and 100 mV, respectively Coupon 35 wire near 100 mV
Immersed Coupons vs. SCE	Two coupons near -325 mV	Three coupons' potentials within ±50 mV
Level 1 Coupons vs. Pt wire	—	Two coupons near 0 mV, third coupon at -300 mV
Level 2 Coupons vs. Pt wire	—	Coupons' potentials range between -228 to -164 mV
Level 3 Coupons vs. Pt wire	—	Coupons' potentials range between -212 to -182 mV

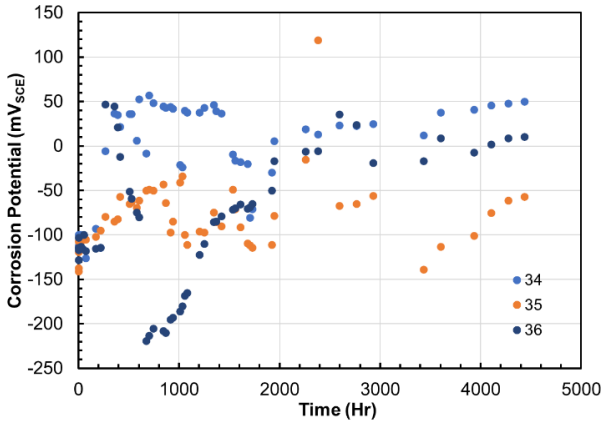

(a) Immersed coupons in GW simulant + VCI-B with respect to SCE

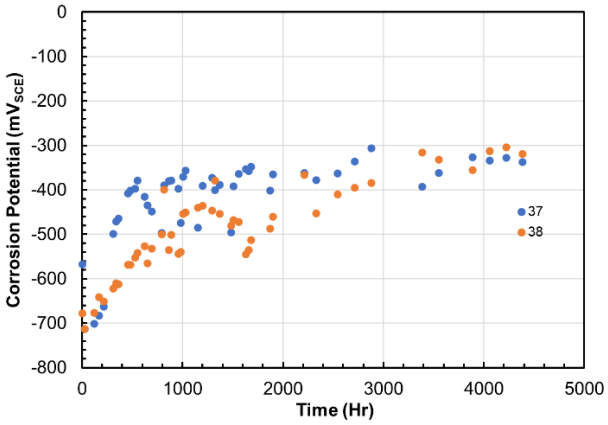

(b) Immersed coupons in GW simulant only with respect to SCE

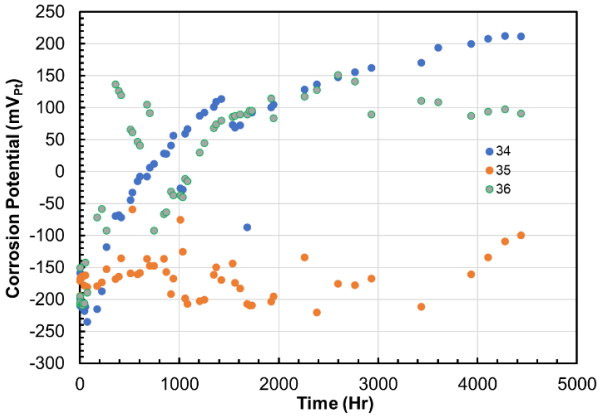

(c) Immersed Pt-wire in GW simulant + VCI-B with respect to SCE

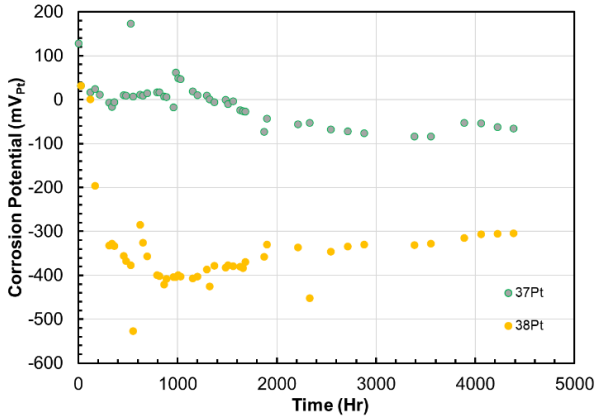

(d) Immersed Pt-wire in GW simulant only with respect to SCE

Figure 6-23. Corrosion potentials of the immersed coupons and Pt-wires with respect to saturated calomel reference electrode.

Regarding the vapor space coupons in Vessel 3, of the three coupons at Level 1, the corrosion potentials of the two coupons are close of 0 mV_{Pt} whereas potential of the third coupon is close to -300 mV_{Pt} after six months of exposure. Similarly, the corrosion potentials of the three Level 2 coupons with respect to Pt wires are in the range of -228 to -164 mV_{Pt}, and corrosion potentials of the Level 3 coupons are in range of -212 to -182 mV_{Pt}. The corrosion potential data of the coupons with respect to the Pt wires indicate that the Pt-referenced corrosion potentials were not stable in vapor phase.

In summary, the immersed coupons' corrosion potentials in GW simulant + VCI electrolyte were distinctly different compared to GW simulant only electrolyte, when measured with respect to the saturated calomel electrode. However, the corrosion potentials of the immersed Pt wires in the two electrolytes overlapped, indicating that Pt wires' potentials were not steady, and Pt wires could not be used as references to measure corrosion potentials of the coupons.

Post-test Images of the coupons exposed to GW simulant + 100% VCI-B (Vessel 3) are presented in Figure 6-24, and post-test profiled images are in Figure 6-25, and corrosion rate data is graphically presented in Figure 6-26. Examination of the profiled images of the coupons showed that deep pits occurred on most of the coupons where Nafion film was used to electrically connect the Pt wire and metal surface in each coupon assembly.

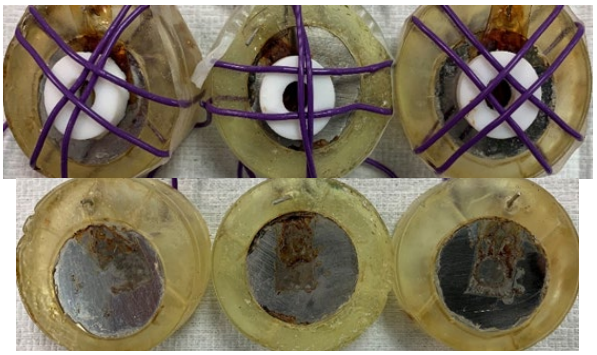

(a) Level 1

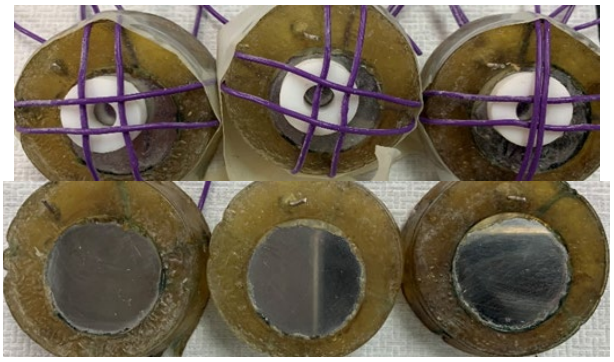

(b) Immersed

Figure 6-24. Post-test images of the coupons exposed to GW simulant + 100% VCI-B in Vessel 3

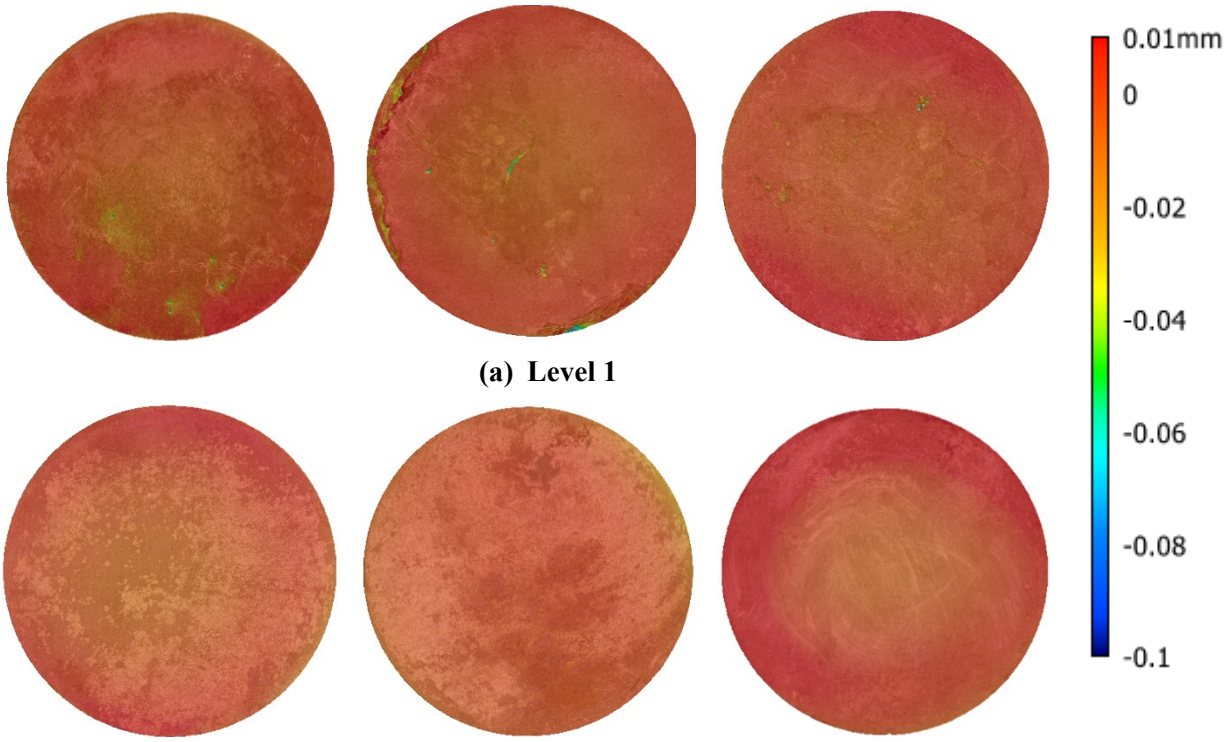

(a) Level 1

(b) Immersed

Figure 6-25. Post-test profiled images of the coupons exposed to GW simulant + VCI in Vessel 3

The post-test images and profiled images of the coupons that were exposed to GW simulant only are presented in Figure 6-27. The coupons in Figure 6-27 were profiled using the same color map scale as in Figure 6-25. Both Vessel 3 coupons were immersed in GW, but only Coupon 38 had Nafion to interconnect the Pt wire and coupon surface. As seen in Figure 6-27, the coupon with Nafion has more concentrated corrosion, directly underneath the Nafion film coverage. The Nafion film pieces were visually examined after the test. It was found that the Nafion film pieces have become more brittle after the tests. This indicated that both physical and chemical properties of Nafion degraded during the GW simulant and GW simulant + VCI exposure tests. Therefore, corrosion rates from all coupons with the Nafion were not considered when evaluating the performance of the coupons in 100% VCI-B for 6 months.

The corrosion rate data of the coupons exposed to GW simulant + 100% VCI-B, immersed and Level 1 is listed in Table 6-9, while the corrosion rates of the coupons exposed to GW simulant only solution, immersed, for six months in Vessel 3 is listed in Table 6-10. The data indicate that there is nearly a 10- to 20- fold decrease in the surface average corrosion rate and a 5- to 10- fold decrease in the pitting rate. This result again emphasizes the effectiveness of the VCIs in mitigating corrosion.

Table 6-9 Corrosion Rates of the Coupons Exposed to GW simulant + VCI-B Solution in Vessel 3

Level	Corrosion Type	Corrosion Rate (mpy)			Average + Std of Surface Average Corrosion Rate (mpy)	Average + Std of Pitting Corrosion Rate (mpy)
		Coupon 1	Coupon 2	Coupon 3		
Level 1	Surface Average	0.82	0.32	0.16	0.34 ± 0.34	8.0 ± 0.7
	Pitting Corrosion	8.7	7.8	7.4		
Immersed	Surface Average	0.19	0.14	0.19	0.17 ± 0.03	1.2 ± 0.2
	Pitting Corrosion	1.3	1.4	1.0		

Table 6-10. Corrosion Rates of the Coupons Exposed to GW simulant Solution in Vessel 3

Coupon Number	Condition	Corrosion Rate
37	Immersed, No Nafion	Surface average corrosion Rate: 8.1 mpy Pitting corrosion rate: 36.4 mpy
38	Immersed, Nafion to connect Pt wire and coupon surface	Surface average corrosion rate: 7.9 mpy Pitting Corrosion Rate: 30.9 mpy

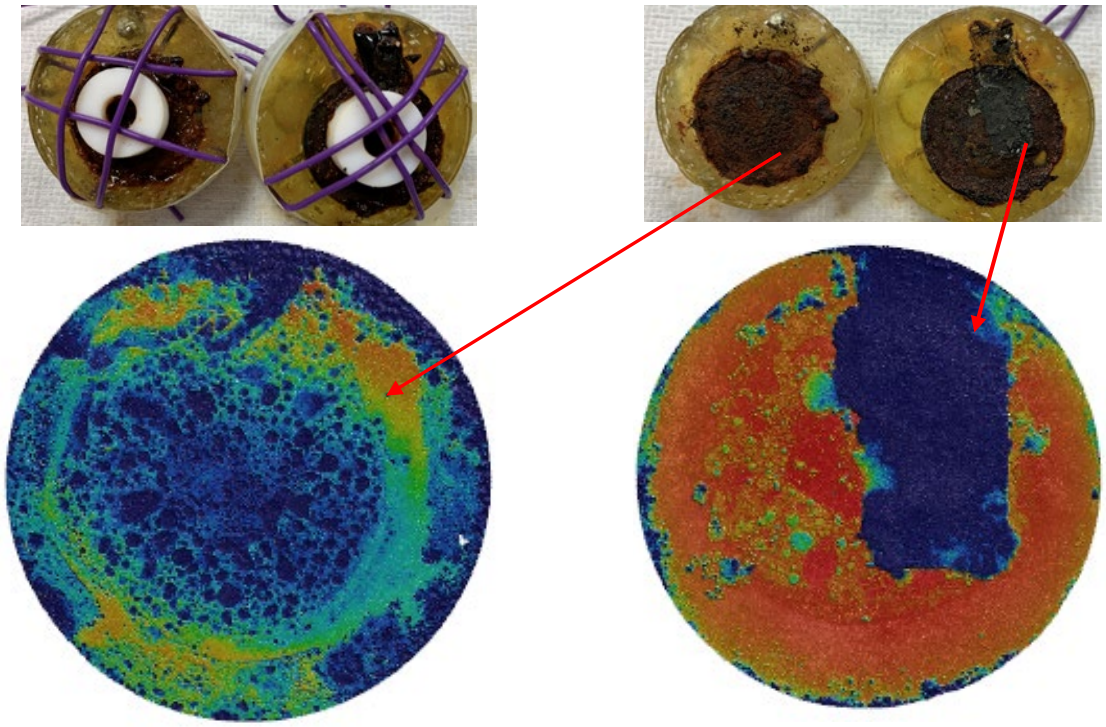

Coupon 37 **Coupon 38**

Figure 6-26. Post-test images and profiled images of the coupons exposed to GW simulant in Vessel 4

6.2.4 Coupling Current Experiments

The results for the coupling current tests are detailed in Table 6-11. The data are also presented graphically in Figures 6-27 and 6-28. In general, the measured corrosion rates were extremely low. In comparison, the corrosion rate of carbon steel in the GW simulants has been observed to be in the range of 3-5 mpy. The coupling current data show that the rates are much less than in the presence of no VCI. Thus, a distributed concentration of the VCIs under the tank bottom is not likely to result in enhanced corrosion.

Table 6-11. Test matrix of the coupling current experiments, terminal coupling current, and corresponding corrosion rates

Experiment No.	Electrolytes	Terminal Coupling Current (mA)	Corrosion Rate Corresponding to Coupling Current (mpy)*
1	Two carbon steel coupons in a beaker filled with GW simulant	~0	~0
2	Electrolytes 1 and 2 being the GW simulant	~0	~0
3	Electrolyte 1: GW simulant dosed with 100% VCI-B, Electrolyte 2: GW simulant	7.1×10^{-3}	0.6
4	Electrolyte 1: GW simulant dosed with 100% VCI-B, Electrolyte 2: GW simulant dosed with 50% VCI-B	5.0×10^{-7}	5×10^{-5}
5	Electrolyte 1: GW simulant dosed with 100% VCI-B, Electrolyte 2: GW simulant dosed with 25% VCI-B	2.5×10^{-7}	2.5×10^{-6}
6	Electrolyte 1: GW simulant dosed with 50% VCI-B, Electrolyte 2: GW simulant dosed with 25% VCI-B	~0	~0
7	Electrolyte 1: GW simulant dosed with 50% VCI-B, Electrolyte 2: GW simulant	2.2×10^{-2}	2
8	Electrolyte 1: GW simulant dosed with 25% VCI-B, Electrolyte 2: GW simulant	1.2×10^{-2}	1.1
Conversion factor: 5.5×10^{-2} mA = 5 mpy			

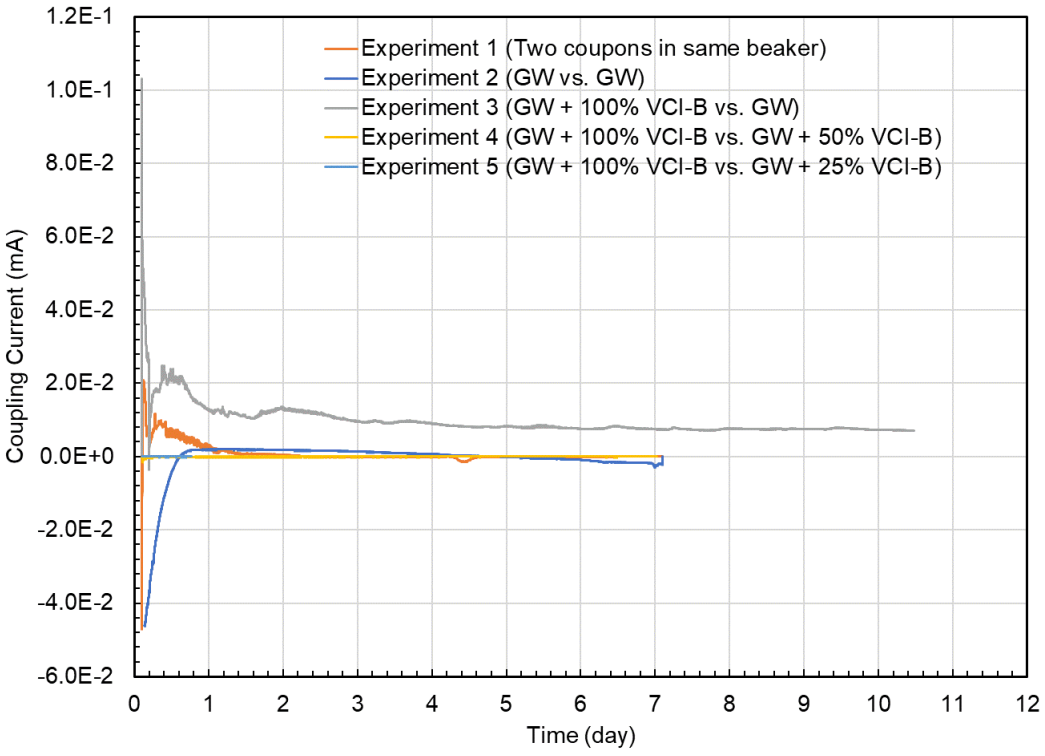

Figure 6-27. Coupling current data for Experiments 1-5.

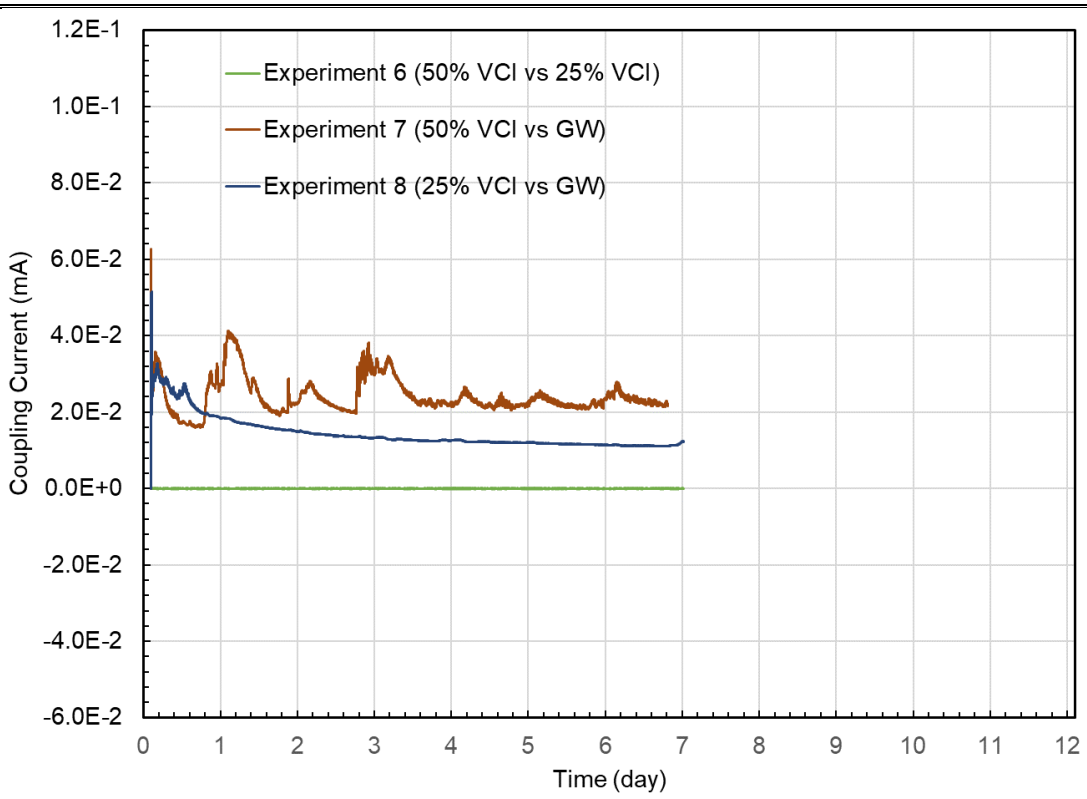

Figure 6-28. Coupling current data for Experiments 6-8.

7.0 Conclusions

Conclusions for activities and experimental tasks that were performed for FY21 supporting Hanford DSTs are presented below in subsections.

7.1 Underdeposit Corrosion Testing

Simulated AZ-101 sludge was prepared, and a method was developed to deposit a dry, adherent sludge layer on the metal coupon surfaces. Electrochemical monitoring utilizing OCP and EIS indicated that the initial adherent, dry sludge layer is not stable after approximately 1 month. Subsequently, the inhibited liquid, which simulated the presence of free liquid in the tank, has free access to the metal surface and passivates the surface. The initial decrease in the OCP for tests with adherent sludge did correlate with the presence of micropits on the coupon surface. However, after approximately 1 month the OCP began to increase and assumed a steady, more anodic value. It is hypothesized that after the breakdown of the sludge layer, that the micropits were passivated. Tests that were performed with loose sludge showed no evidence of micropits and OCP measurements indicated that the potential increases in the anodic direction from its initial value.

7.2 Secondary Liner Corrosion

The two- and six-month coupon data collected in GW only simulant indicated that aggressive corrosion continues even after the first two months of exposure. This result indicated that VCIs may effectively mitigate corrosion of the secondary liners at the Hanford site. In addition, the tests with 25% of the recommended VCI-B dosage showed that the inhibitor ceases to be effective at the 25% level. Based on previous results from testing in FY19 and FY20, the threshold minimum dosage for VCI-B is between 25 and 50% of the recommended dosage. In practice, if the concentration of VCI-B decreased below 50%, it is likely that replenishment of the VCI would be necessary.

Determining migration rates of the VCIs is critical to field implementation of the VCI technology. It was hypothesized that corrosion potential data can be used to study and determine migration of VCIs. A Pt-wire embedded in each coupon assembly was used as a reference for the vapor space and immersed phase coupons in GW simulant + VCI-B and GW simulant only electrolytes. A saturated calomel electrode was also used as the reference for the immersed coupons. The immersed coupons' corrosion potentials in GW + VCI electrolyte were distinctly different compared to GW simulant only electrolyte, when measured with respect to the saturated calomel electrode. However, the corrosion potentials of the immersed Pt wires in the two electrolytes overlapped, indicating that Pt wires' potentials were not steady, and Pt wires could not be used as references to measure corrosion potentials of the coupons. Although, accurate potential data were not gathered from this test, corrosion rates from 6-month tests with carbon steel exposed to GW+VCI-B and GW only simulants were able to be compared. The results indicated that there is nearly a 10- to 20-fold decrease in the surface average corrosion rate and a 5-to 10- fold decrease in the pitting rate. This result again emphasizes the effectiveness of the VCIs in mitigating corrosion.

The coupling current tests showed that a distributed concentration of the VCIs under the tank bottom is not likely to result in enhanced corrosion. The corrosion rate of carbon steel in the GW simulants has been observed to be in the range of 3-5 mpy. The coupling current data in general show that the rates are much less than in the presence of no VCI. Thus, a distributed concentration of the VCIs under the tank bottom is not likely to result in enhanced corrosion.

7.3 Recommendations for FY22 Testing

Recommendations for follow-on work are summarized below. These recommendations were incorporated into a proposal for FY22 activities.

Underdeposit Corrosion

- Investigate underdeposit corrosion under the non-porous adherent deposits considering the effect of water content.

Secondary Liner

- Explore alternative corrosion mitigation methods such as nitrogen blanketing that will effectively de-aerate the system.

8.0 References

[1] R. E. Fuentes, P. K. Shukla and B. J. Wiersma, "Task Technical and Quality Assurance Plan for Hanford Double Shell Waste Tank Corrosion Studies-FY21", SRNL-RP-2021-00178, Savannah River National Laboratory, Aiken, SC, March 2021.
[2] T. J. Barnes, K. D. Boomer, J. R. Gunter, and T. J. Venetz, "241-AZ Tank Farm Construction Extend of Condition Review for Tank Integrity", RPP-RPT-54818, August 1, 2013.
[3] "Double-Shell Tank Tertiary Leak Detection System Evaluation", RPP-RPT-55666, Rev. 3, 2016

[4] R. E. Fuentes. B. J. Wiersma and K. Hicks, "Hanford Double Shell Waste Tank Corrosion Studies-Final Report FY14", SRNL-STI-2014-00616, Savannah River National Laboratory, Aiken, December 2014.
[5] R. E. Fuentes and R. B. Wyrwas, "Hanford Double Shell Waste Tank Corrosion Studies-Final Report FY15", SRNL-STI-2016-00117, Savannah River National Laboratory, Aiken, May 2016.
[6] R. E. Fuentes, "Hanford Double Shell Waste Tank Corrosion Studies-Final Report FY16", SRNL-STI-2016-00721, Savannah River National Laboratory, Aiken, February 2017.
[7] R. E. Fuentes, "Hanford Double Shell Waste Tank Corrosion Studies-Final Report FY17", SRNL-STI-2018-00116, Savannah River National Laboratory, Aiken, April 2018.
[8] R. E. Fuentes, P. K. Shukla, B. Peters, D. A. Hitchcock, "Hanford Double Shell Waste Tank Corrosion Studies-Final Report FY2018", SRNL-STI-2019-00014, Savannah River National Laboratory, Aiken, August 2019.
[9] R. E. Fuentes and P. K. Shukla, "Hanford Double Shell Waste Tank Corrosion Studies-Final Report FY2019", SRNL-STI-2020-00109, Savannah River National Laboratory, Aiken, July 2020.
[10] P. K. Shukla, et al., "Vapor Corrosion Inhibitors Effectiveness for Tank Bottom Plate Corrosion Control", PRCI, Inc. Report Catalog Number PR-015-153602-R01, 2018.
[11] P. K. Shukla, R. E. Fuentes, B. J. Wiersma, "Hanford Double Shell Waste Tank Corrosion Studies-Final Report FY2020", SRNL-STI-2021-00142, Savannah River National Laboratory, Aiken, July 2021.
[12] ASTM A515, "Standard Specification for Pressure Vessel Plates, Carbon Steel, for Intermediate- and Higher-Temperature Service", ASTM International, West Conshohocken, PA, 2003.

[13] RPP-RPT-42921, November 1999.
[14] Personal communication from L Stock, “AZ-101 Simulant June 3”, June 2, 2020.
[15] R. E. Eibling, R. F. Schumacher, and E. K. Hansen, “Development of Simulants to Support Mixing Tests for High Level Waste and Low Activity Waste”, WSRC-TR-2003-00220, December 2003.
[16] G. H. Beeman, “Composition of AZ-101 Envelope D and Associated Wastes, RPP-WTP-02-168, RPP-WTP-02-184, RPP-WTP-02-199, Battelle-Pacific Northwest Division, Richland WA 99352 (June 21, 2002), (July 31, 2002), (September 5, 2002).
[17] Private communication D. Lambert, M. Stone, and M. Siegfried on November 18, 2021.
[18] K. J. Cantrell, R. J. Serne, and G. V. Last, “Hanford Contaminant Distribution Coefficient Database and Users Guide”, PNNL-13895, Rev. 1, June 2003.
[19] ASTM G1-03 “Standard Practice for Preparing, Cleaning, and Evaluating Corrosion Test Specimens”, ASTM International, West Conshohocken, PA, 2011.
[20] ASTM G5-13 “Standard Reference Test Method for Making Potentiodynamic Anodic Polarization Measurements”, ASTM International, West Conshohocken, PA, 2013.
[21] T. Martin, “Outcomes from the August 2013 Expert Panel Oversight Committee Meeting,” RPP-ASMT-56781, Washington River Protection Solutions LLC, Richland, WA, February 2014.

Appendix A Chemical Composition of Simulants used in Secondary Liner Corrosion Testing

Table A-1 Composition for GW simulant

Temperature	45	°C
pH adjusted	7.6	
Volume	2	L

Simulant Source	Formula	Concentration (M)	Weight required (g)
Sodium bicarbonate	$NaHCO_3$	1.750E-03	0.2940
Calcium hydroxide	$Ca(OH)_2$	1.500E-03	0.2223
Potassium nitrate	KNO_3	2.400E-04	0.0485
Ferric sulfate	$Fe_2(SO_4)_3$	6.250E-04	0.4999
Ferric chloride	$FeCl_3$	7.667E-05	0.0249
Strontium Nitrate	$Sr(NO_3)_2$	2.874E-06	0.0012
Sodium Metasilicate, 5-hydrate	$Na_2SiO_3.5H_2O$	6.000E-04	0.2546
Magnesium Chloride	$MgCl_2$	3.100E-04	0.0590
Acetic Acid	$C_2H_4O_2$	3.000E-04	0.0360

Appendix B Pictures of Secondary Liner Corrosion Testing Samples after Test

Samples cold mounted

Vessel 1: Groundwater Control Test: Level 3
6 months

Vessel 1: Groundwater Control Test: Level 2
6 months

Vessel 1: Groundwater Control Test: Level 1
6 months

Vessel 1: Groundwater Control Test: Immersed

6 months

Samples cold mounted

Vessel 2: Groundwater with 25% VCI: Level 3

2 months

6 months

Vessel 2: Groundwater with 25% VCI: Level 2

2 months

6 months

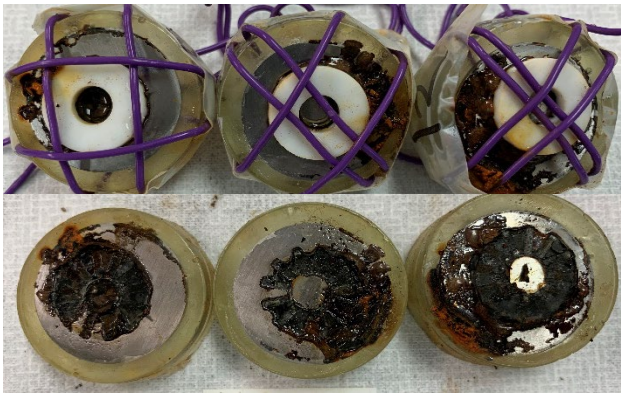

Vessel 2: Groundwater with 25% VCI: Level 1

2 months

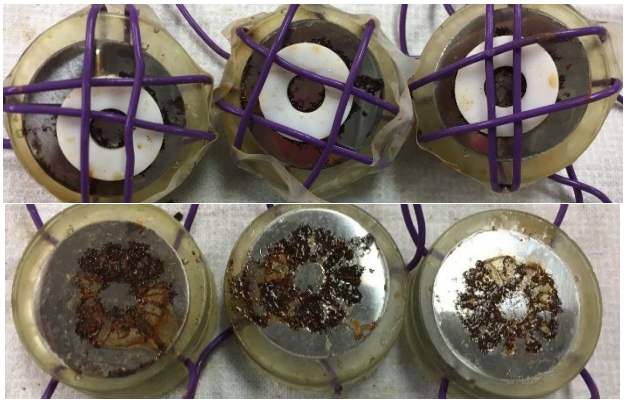

6 months

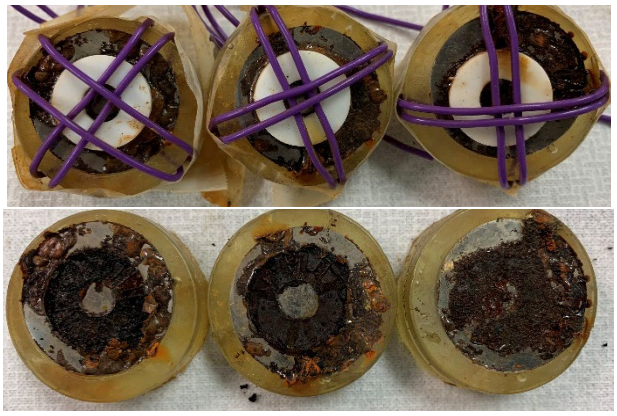

Vessel 2: Groundwater with 25% VCI: Immersed

2 months

6 months

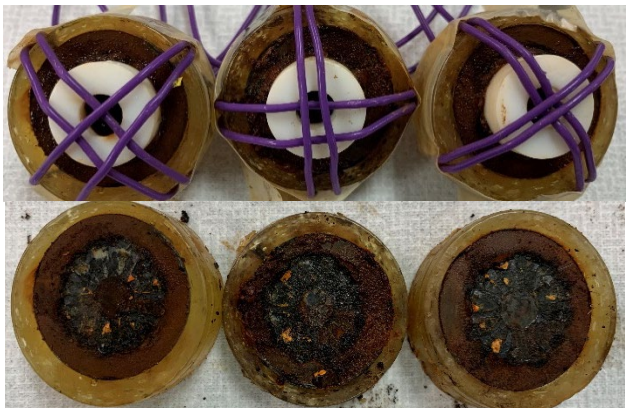

Samples cold mounted

Vessel 3: Groundwater with 100% VCI: Level 3
6 months

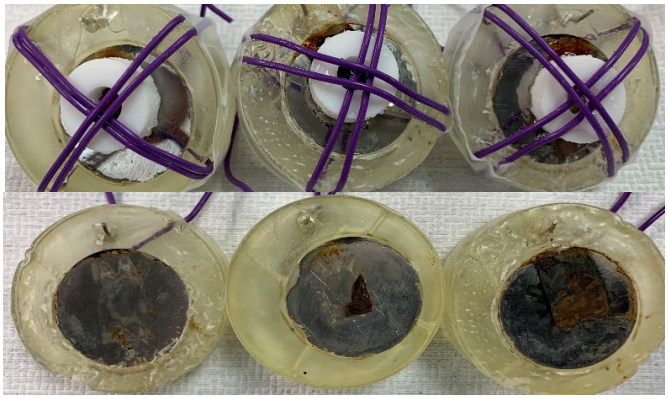

Vessel 3: Groundwater with 100% VCI: Level 2
6 months

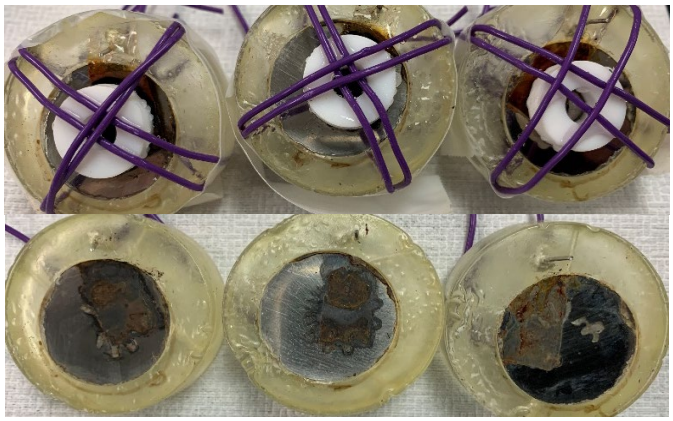

Vessel 3: Groundwater with 100% VCI: Level 1
6 months

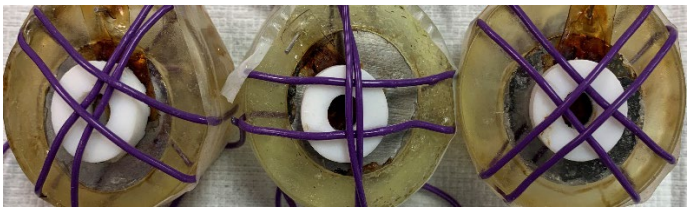

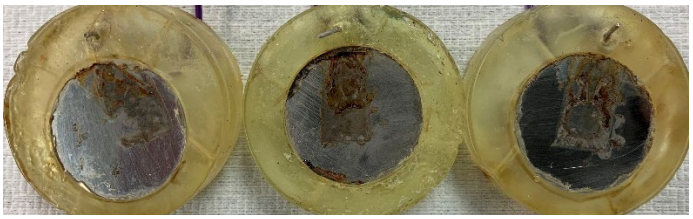

Vessel 3: Groundwater with 100% VCI: Immersed
6 months

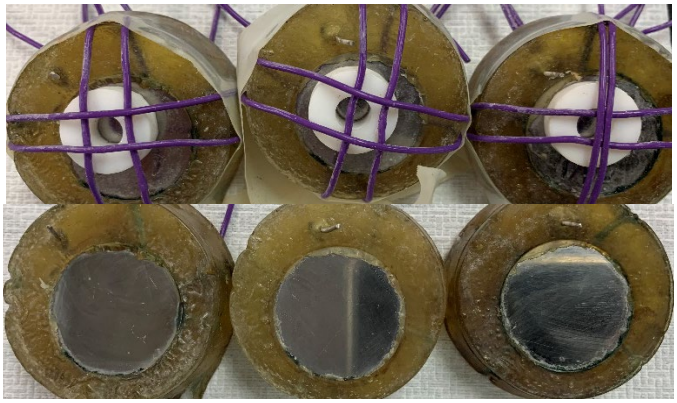

Samples cold mounted

Vessel 4: Groundwater: Immersed
6 months

Distribution

alex.cozzi@srnl.doe.gov
joseph.manna@srnl.doe.gov
connie.herman@srnl.doe.gov
crystal_l_girardot@rl.gov
eric.skidmore@srnl.doe.gov
jason_s_page@rl.gov
Joshua.boerstler@srnl.doe.gov
michael.stone@srnl.doe.gov
Records Administration (EDWS)
Richard.wyrwas@srnl.doe.gov
robert_j_nelson@rl.gov
shawn_t_campbell@rl.gov
jason_r_gunter@rl.gov
kayle_d_boomer@rl.gov
matthew.siegfried@srnl.doe.gov